HIGHWAY RESEARCH RECORD

Number 389

Concrete Pavement Construction and Joint Sealants

6 reports
prepared for the
51st Annual Meeting

Subject Areas

26 Pavement Performance
33 Construction
34 General Materials

HIGHWAY RESEARCH BOARD
DIVISION OF ENGINEERING NATIONAL RESEARCH COUNCIL
NATIONAL ACADEMY OF SCIENCES—NATIONAL ACADEMY OF ENGINEERING
Washington, D.C. 1972

FOREWORD

The first three papers in this RECORD will be of interest to researchers, designers, specification engineers, and contractors concerned with the design and construction of portland cement concrete pavements. The paper by Scholer and Olateju, extracted from an earlier report, reviews in detail the currently available methods for mechanical placement of steel for continuously reinforced concrete pavements constructed using the slip-form method. A time-lapse photography technique was utilized to evaluate the various placement methods.

Various texturing methods were explored by Chamberlin and Amsler to determine their effects on the depth, uniformity, and durability of the texture in addition to the effect on skid resistance. The study indicates a definite correlation between texture depth and skid resistance. An unconventional fluted float was found to provide a deep texture that had high skid resistance, was more uniform, and appeared to wear at a lower rate than other textures studied.

A 900-ft section of 2-lane highway constructed of precast, prestressed concrete panels being tested in South Dakota is reported by Larson and Haug. The paper gives a brief account of the technique utilized in the construction of the pavement. The 6-ft wide, 24-ft long and $4\frac{1}{2}$-in. thick panels were overlaid with a bituminous mat and are being evaluated for structural performance. A cost summary of this unique pavement, which may have potential for future highway use, is reported.

The remaining papers in this RECORD deal with pavement joint seals and will be of interest to researchers, designers, materials engineers and contractors concerned with improving the performance of concrete pavement joint seals. Gaus cites the need for a long-term performance type of sealant for new construction and maintenance of joints in concrete pavements. He reports on experiences beginning in 1963 with the use of PVC elastomeric hot-poured sealants.

Brown reports the observations made during a survey of neoprene compression seals and other joint sealing systems in five states. The report concludes that only the neoprene seals, by keeping incompressible materials and liquids from the joints, provide satisfactory performance and extend the life of the pavement. Neoprene seals have also prevented blowups in the pavements surveyed.

The development of a simple viscoelastic model to simulate the time-dependent behavior of elastomeric seals is reported by Vyas. The response of the model is compared with that observed for the seal to verify the adequacy of the model. It was found that viscoelastic models can be effectively used to represent elastomeric seals.

—John C. Dixon

MECHANICAL METHODS OF STEEL PLACEMENT FOR SLIP-FORM CONSTRUCTION OF CONTINUOUSLY REINFORCED CONCRETE PAVEMENTS

C. F. Scholer and O. T. Olateju, Purdue University

•TRADITIONAL methods for the incorporation of steel in concrete pavement slabs have included the use of chair supports, "two-lift" placement with the reinforcement sandwiched between two layers of concrete, and movable sled devices that are used to hold the steel at predetermined heights and are rolled away as the concrete is poured. The rate at which steel could be placed by any of these methods was not compatible with the inherent production capabilities of the slip-form paver. Consequently, during the past several years, major efforts have been directed toward the development of mechanical methods for placing mesh or reinforcing bars or both in conjunction with slip-form paving. Today, because of these improved devices, contractors can lay 6,000 ft or more of reinforcement in less than 10 hours.

The mechanical devices for steel placement in pavement slabs can be categorized into two general groups: the mesh depressors and the bar placers.

MESH DEPRESSORS

The mesh depressor was the first breakthrough in the search for machines to place reinforcement in one lift. It was used in Oregon (1960), Louisiana (1961), and Indiana (1962). The early version of this unit rode on forms and used vibration and pressure to depress the steel. The unit depressed the steel while standing stationary, which precluded the lateral displacement of the mesh during depression. The machine was self-propelled and carried four hydraulic rams under which was suspended a lattice steel frame. On the frame at each ram was a vibrator. Limit chains were used to halt the frame at the correct depth for mesh embedment. The rams then retracted the frame in preparation for the next sinking cycle. Another version, used in Indiana in 1962, consisted of a giant screen or grid that vibrated and depressed the sheet of mesh fabric to its proper depth. The steel placement unit was fitted with large depressing units that left a waffle pattern on the concrete. Its pressing depth was governed by adjustable locknuts on threaded guide rods instead of by limit chains.

At the time of this study, the manufacturers of mechanical mesh depressors were Heltzel Steel Form Co., Rex Chainbelt Co., and CMI, Inc. Each of these companies produces a single model that can be used either with side-form or with slip-form paving. The machine made by the Heltzel Co. is a self-propelled unit, whereas the other two machines are attachments to slip-form pavers, spreaders, or finishers.

The Heltzel Co. unit is adjustable in width from 12 to 24 ft and carries four grids with vibration runners on 20- by 23-in. centers Each grid consists of four blades welded to the vibrator housing. The basic length of the grid is 10 ft.; it can be extended to 15 ft by using detachable end sections. The machine depresses steel from the surface of the full depth slab. Mesh is placed on the surface of the wet slab, and the machine moves forward to position directly over the mesh. As the mesh depressor comes to a full stop, its operator actuates the vibration grids and the hydraulic pressure. Vi-

Sponsored by Committee on Rigid Pavement Construction.

bration and pressure are the major factors responsible for sinking the mesh. Vibration helps to move the aggregate particles aside while the wire moves down into the mix. After the mesh has been depressed to the proper depth, hydraulic cylinders lift the grids from the concrete and the machine moves to the next position. The operation of depressing the steel takes between 10 and 18 sec and leaves a waffle pattern on the slab. Although the machine stands squarely on the mesh that is being depressed, a length of 1 ft or more of the next mesh section at the point of overlap is also depressed. This eliminates the possibility of the next sheet being dragged as the machine moves forward. It also eliminates the need for more extensive vibration of the concrete after the initial depression cycle.

The current model of the Rex Chainbelt unit was introduced in 1965. This unit rides on crawler tracks as an attachment to the front of a placer or slip-form paver. It consists essentially of a set of blades, in two banks, that are attached to a frame. A mechanism of gears and springs within this frame produces an eccentric movement with an amplitude of $\frac{3}{4}$ in. This arrangement imparts an oscillatory motion to the blades, and the resulting tamping and tucking action makes continuous steel placement possible without vibration. The final depth for the steel depends on the setting of the rear ends of the blades. Both the blades and the slopes can be adjusted to meet the paving conditions encountered. The depressor blades are evenly spaced across the full slab width and can depress mesh to depths of 6 in. The depressor units are hydraulically lifted to pass over dowel brackets, and crown adjustments are made from the slip-form or placer console.

The unit manufactured by CMI, Inc., also attaches to the front of a slip-form paver. It depresses the mesh into the mix by using high-frequency vibration and low amplitude. The blades are vibrated at 2,000 to 4,000 cpm with an amplitude of $\frac{1}{8}$ in. Vertical baffles are responsible for pushing the steel into the concrete. The machine rides on pneumatic tires and is hydraulically powered from the slip-form unit. It is equipped with side forms to keep the mix within the paving boundaries while the steel is being depressed.

BAR PLACERS

Where bar mats and mesh are used, most of the labor is performed in the shop, and relatively few workers are required in the field. Where reinforcing bars are used, however, workers are required to load and unload the steel and to distribute and tie it. Contractors have therefore developed machines that help to speed the lapping and tying. They have also developed machines that will hold the tied steel in the desired position for pavement construction. Either this position can be the final one, in which case the concrete is placed through and around steel, or the steel can be placed on the surface of the fresh concrete and then depressed to its final position. Three distinct types of equipment can be identified within the bar placer group.

Bar Vibrator Machine

The bar vibrator unit is decreasing in popularity because it is not adaptable for use with the slip-form paver. It is similar in design to the mesh depressor of the Heltzel Co., except that notches are used under the grid to hold the steel bars in their proper position.

In 1964, two Illinois contractors used two machines to place reinforcing bars by a method that eliminated chair supports and permitted single-lift paving. The first machine was a riding platform, 45 ft in length, that traveled behind a concrete spreader. This unit was manned by workers who took bundles of 30-ft long bars from delivery cranes and strung them out in position, spliced and wire tied them, and fed the bar lines into a set of spacing cups. The steel drew itself off as the rig advanced. Transverse bars were placed on 25-in. centers by two reels mounted in front of the machine. These transverse bars were positioned on the longitudinal bars.

The second machine, which performed the actual depressing of the steel, consisted of two 12- by 15-ft assemblies of large vibrating grids. After the machine was moved into position over the slab, a hydraulic ramp depressed the bars a distance of 15 ft.

Grooved surfaces distributed the ram pressure over the steel and ensured its even submergence without local distortion or major disturbance of the fresh concrete.

Tube Assembly

The assembly holds the reinforcement in position while the concrete is deposited, spread, and consolidated. It consists of a form-riding frame that contains flared tubes for receiving and positioning the steel just ahead of the concrete spreader. Two modifications of this machine are currently in use. In the first, 44 or 48 lines of reinforcement are fed through the tubes. In the second, the middle 6 bars are not positioned but instead are supported with tie bars on chairs. The first type has recessed tubes, whereas the second type has tubes of equal length.

The first step in the paving operation is to lay the lapped and tied steel reinforcement out on the subgrade. The steel is then fed individually through flared tubes that are 16 to 30 ft in length. There are either 44 or 48 tubes, depending on the design spacing of the longitudinal bars. The outside diameter of the flares is about 3 in. and the inside diameter of the tubes is $2\frac{1}{2}$ in. After bar feeding has been accomplished, the unit is attached to the front of the concrete placer where it is held at the proper elevation while the concrete is placed and consolidated. The height of the tubes can be adjusted with the aid of double nuts and bolts that are located in the top of the attaching beam in the rear; another set of double nuts at the bottom can be used to adjust the tubes horizontally. The unit itself is controlled from the operator's console. One version now in use has hydraulic cylinders at each corner to control the height. The frame holding the tubes is hinged on the bottom at the centerline of the roadway with a hydraulic cylinder on top of the hinged portion. This center cylinder raises the tubes to the desired straight-line crown. Tie bars, depending on their position, can be inserted by hand or by rotating the notch drum at the back of the placer. They can also be supported on chairs.

Rebar Installer

The installer was introduced by the Rex Chainbelt Co. in 1969. It was designed to be compatible with the company's belt placer although it can be used with the slip-form paver. It consists of four drums. On each drum is mounted a set of helical rows of teeth like those on a mower sickle bar. The drums span the entire width of the slab and are mechanically operated. They are designed to slowly rotate while the individual bars are gradually tamped downward to the desired position. The drums operate independently of each other and are hydraulically controlled from the slip-form console.

The paving operation is started by laying, lapping, and tying continuous lengths of reinforcing rods on the subgrade. There is no need to line up the rods accurately. The steel is then raised above the subgrade by a roller in front of the spreader and is threaded to the belt placer in two separate sets. The steel goes over the belt spreader and out through the back. A rubber-tired unit attached to the trailing forms of the spreader brings the two sets of steel together and roughly spaces them across the width of the pavement. This unit has two horizontal pipes between which is a series of short vertical rollers, placed at either 6 or $6\frac{1}{2}$ in. depending on the number of lines of steel bars (usually 40 or 48 lines). The rods are fed through these rollers for proper spacing.

Another spacing unit, similar in design to the other spacer, is attached to the slip-form paver. Here, all the bars are properly spaced and held in position by the set of vertical rollers. This unit is followed by track-mounted, saw-toothed rotary tampers that are attached to the front of the slip-form paver. As the machine advances, the drums revolve, and the serrations slip over the rods and force them down into the fresh concrete. Because the rebar installer is attached to a slip-form paver and takes its grade from the paver wires, it installs the steel precisely to the desired elevation.

SUMMARY OF FINDINGS

The extent of the use of mechanical steel placers in this country was evaluated through questionnaires directed to selected highway officials, correspondence and in-

terviews with contractors and other highway officials, and observations of actual jobs. The procedures followed on selected jobs were recorded on film with the aid of a time-lapse camera, and the photographs were later used in the analyses of the placement methods and techniques. From the observation and the subsequent analyses, the following summary comments are made:

1. The number of states that have turned to the use of continuously reinforced concrete pavements is rapidly increasing.
2. Machines are now available that can place steel faster, at less expense, and with less labor than the manual operations formerly employed. These machines have been used to the general satisfaction of the state highway officials.
3. Several states have modified their specifications so as to accommodate placement tolerances that are compatible with the mechanical methods.
4. Many states have eliminated the use of transverse bars in the construction of continuously reinforced concrete pavements.
5. Through adequate planning and the use of mechanical methods for steel placement, contractors have demonstrated that they can improve the efficiency of their steel laying operations.
6. Currently available mechanical devices for depressing steel are not yet fully perfected, but additional improvements can be expected in the future.
7. The savings that can currently be realized from the use of mechanical steel placers cannot be specifically identified because of limited experience. However, the potential savings can be sufficiently attractive to warrant the interest of highway officials.

ACKNOWLEDGMENT

The information contained in this paper was extracted from a report entitled Techniques in Slip-Form Paving and Continuously Reinforced Concrete Pavement Construction (Joint Highway Research Project Report No. 6). This report is available through the School of Civil Engineering at Purdue University.

PILOT FIELD STUDY OF CONCRETE PAVEMENT TEXTURING METHODS

W. P. Chamberlin and D. E. Amsler, New York State Department of Transportation

The effect of different texturing methods on texture depth, initial skid resistance, texture uniformity, and texture durability was studied through a designed field experiment installed at five different locations. The textures studied included those produced by three conventional methods (burlap drag, natural-bristle broom, and wire broom) and one unconventional method (fluted magnesium float). The latter method produced uniform, parallel, $\frac{1}{8}$-in. deep, semicircular ribs on $\frac{3}{8}$-in. centers. All textures were placed perpendicular to the centerline of the pavement. Textures produced by the fluted float were found to be deeper and to provide greater skid resistance than textures produced by the burlap drag or the natural-bristle broom. They were equivalent in these respects to those produced by the wire broom but were found to be more uniform and to wear at a slower rate. It was concluded that more consideration should be given to the merits of such geometrically definable textures and that the relationships among texture geometry, skid resistance, and abrasion resistance should be the subjects of more research.

•THE skid resistance of a concrete pavement—defined for this discussion as tire-pavement friction in the locked-wheel mode (1, pp. 11-13)—results from a combination of intrinsic and extrinsic factors. Of principal importance among the former is the texture of the pavement surface itself, which results from the distribution of asperities of various sizes and shapes over the surface. It has been accepted that pavement designed for high-speed travel should have a texture composed of both fine and coarse asperities because both contribute—although differently—to tire-pavement friction. [A comprehensive discussion of the mechanism of this friction is given elsewhere (1).]

Coarse asperities, which are responsible for what has been called macrotexture or macroroughness, can be controlled by the engineer because they are primarily a function of the method used to texture the pavement surface. In addition to contributing directly to tire-pavement friction, coarse asperities (macrotexture) provide channels for the drainage of water trapped between a pavement and a moving tire. Hydrostatic pressure and skid resistance are dependent on the extent to which water is prevented from draining during the tire-pavement contact period. If hydrostatic pressure develops to the extent that the tire is supported entirely by water film, hydroplaning (the complete loss of interfacial friction) results.

Because of the increasing volumes of high-speed traffic and the growth of interest in the skid resistance of pavements, there has been a tendency to use texturing methods that create deep textures. Not only do these textures have great inherent resistance to skidding, but also they drain well.

The purpose of this paper is to describe the partial results of a pilot field study of four different concrete pavement texturing methods. Data are presented regarding the

Sponsored by Committee on Rigid Pavement Construction.

initial texture and skid resistance of the experimental pavements, and the relative durability of the textures themselves are tentatively evaluated.

STUDY SCOPE AND PROCEDURES

During the 1969 construction season, a designed experiment was built in new pavements at five different sites in New York State. Two specific objectives of the experiment were to determine the initial depth and skid resistance of textures produced by different texturing methods under conditions of field control and to evaluate the relative durability of the textures under the abrasive action of traffic. A third objective was to determine whether a measure of texture depth could be correlated with locked-wheel skid resistance for a variety of texturing methods combined.

The four texturing methods employed were as follows:

1. Burlap drag—typical of that commonly used in the United States and in New York State prior to 1969;
2. Natural-bristle broom—typical of that used in New York State since 1969 and gaining popularity throughout the United States;
3. Wire broom—widely used in England and elsewhere in the British Commonwealth; and
4. Fluted magnesium float—a device that produces a uniform surface of parallel, semicircular ribs on $^3/_8$-in. centers with $^1/_8$-in. penetration.

The first three are conventional methods and were selected to represent the range of current practice in the United States and abroad. The fourth is an unconventional method; i.e., to the authors' knowledge, it had been used only experimentally on two bridge decks in New York State. The details of each method are given in the Appendix, and profiles of representative textures are shown in Figure 1.

Each of the four methods was used on two 120-ft long test sections (A and B) that were placed in the driving lane of pavements at five different sites. The sites selected included a variety of concrete materials and traffic characteristics. All experimental textures were manually placed perpendicular to the pavement centerline at all sites by the same personnel. Details of the sites are given in Table 1, and the data collected at the time of placement are given in Table 2.

Texture depth and skid resistance in the wheelpaths were measured immediately after construction and periodically since then. Texture depths were measured by the sand-patch method (2) after the residual curing compound was removed. Skid tests were performed at speeds of 40 and 55 mph with a locked-wheel trailer in accordance with ASTM Designation E 274-65T. Trailer tires conformed to ASTM Designation E 249-66.

TEST RESULTS

The experiment involving initial textures was designed for a two-factor, four-level (texturing methods) by five-level (sites) analysis of variance with single replication (3). Independent analyses were made for initial texture depth and initial skid resistance at speeds of 40 and 55 mph. In each case, the method of texturing was found to produce a significant effect. Similarly, mean texture depth and skid resistance at speeds of 40 and 55 mph were found to differ significantly from site to site for the same texturing method. No significant interaction was found between methods and sites. Analysis for the components of variance (Table 3) indicated that 68 to 79 percent of the total variance encountered in texture depth and skid resistance was associated with site-to-site and method-to-method effects combined. The results of all initial measurements on the experimental textures are given in Tables 4 and 5.

Subsequent measures of texture depth have shown that the experimental textures wear at a rate dependent primarily on the level of traffic, the initial texture depth, and the method of texturing employed (Table 6).

Variations in the level of texture depth and skid resistance that occurred from site to site for the same texturing method have not yet been fully studied and thus are not included here. Their importance, however, should not be minimized.

Figure 1. Transverse profiles of study textures.

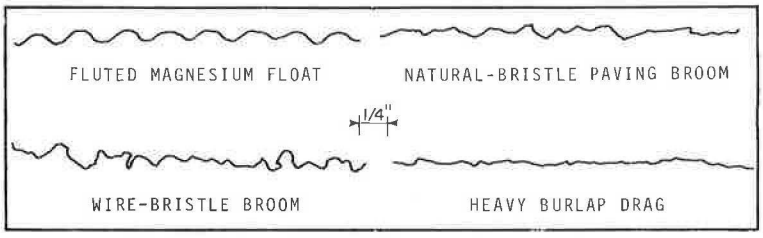

Table 1. Study sites.

Site	Driving Lane AADT Total	Driving Lane AADT Trucks (percent)	Speed Limit (mph)	Estimated Studded Tire Use[a] (percent)	Remarks
1	1,410	1.0	50	30	Most vehicles gradually accelerating or decelerating
2	1,200	5.0	55	40	Pavement snow-packed up to 3½ months each year
3	1,710	4.0	60	40	Most vehicles gradually accelerating
4	5,160	1.0	65	35	—
5	1,870	10.0	60	30	—

[a]Legal between October 15 and May 1.

Table 2. Weather conditions and concrete properties at time of test section placement.

Site	Test Section	Date Placed (1969)	Weather Conditions at Site: Temperature (F)	Relative Humidity (percent)	Clouds (percent)	Wind Velocity (mph)	Concrete Properties: Mean Slump (in.)	Mean Air Content (percent)	Proctor Penetration[a]
1	A	8/14	86	47	0	0-5	2.5	5.7	500 psi at 2½ hr
	B	9/24	67	32	50	0-5	2.4	5.4	—
2	A	7/31	75	70	0[b]	0-5	1.5	4.3	500 psi at 3½ hr
	B	8/1	78	64	0[b]	0-5	1.5	5.2	500 psi at 3 hr
3	A	8/11	82	50	50	16-25	1.8	6.3	500 psi at 3 hr
	B	8/12	78	45	0	16-25	1.5	5.9	460 psi at 2¾ hr
4	A	9/25	55	67	100	0-5	2.5	6.0	160 psi at 6½ hr
	B	9/29	50	52	50	0-5	2.5	6.0	—
5	A	10/30	46	36	0	0-5	2.3	5.3	—
	B	10/30	46	37	0	0-5	2.4	7.7	—

[a]ASTM Designation C 403-65T.
[b]Haze.

Table 3. Percentage of contribution of components to total observed variance.

Source of Variance	Dependent Variable: Texture Depth	Skid Number at 40 mph	Skid Number at 55 mph
Texturing methods	54.2	21.7	40.1
Sites	24.3	55.9	28.0
Site-method interactions	10.2	5.6	8.1
Sampling error	11.2	8.3	13.7
Testing error	0.1	8.5	10.1
Total	100.0	100.0	100.0

Table 4. Summary of initial texture depths.

Site	Test Section	Initial Texture Depth (in. x 10^3): Burlap Drag	Bristle Broom	Wire Broom	Fluted Float	Within-Site Avg
1	A	13.3	26.3	53.3	30.3	
		22.2	28.0	44.3	57.3	
		38.7	31.5	57.3	48.3	
	B	17.0	46.7	53.5	27.3	
		27.0	29.0	40.3	37.8	
		31.3	31.2	22.3	35.7	
	Avg	24.9	32.1	45.2	39.5	35.4
2	A	18.3	23.8	40.0	44.7	
		17.3	26.8	22.3	48.8	
		19.5	27.7	36.5	50.1	
	B	15.0	23.2	49.7	48.0	
		14.3	24.5	30.2	49.2	
		14.8	20.0	17.8	50.5	
	Avg	16.5	24.3	32.8	48.6	30.5
3	A	12.2	24.3	37.5	34.3	
		12.6	18.5	46.7	34.2	
		14.0	13.7	38.5	34.8	
	B	11.7	27.2	31.5	44.0	
		15.8	21.3	24.2	26.5	
		8.0	15.2	39.7	49.3	
	Avg	12.4	20.0	36.4	37.2	26.5
4	A	12.3	48.0	20.0	45.5	
		15.5	26.3	38.8	53.7	
		11.2	38.7	36.8	38.7	
	B	16.5	30.2	34.3	47.5	
		17.7	41.8	21.7	41.0	
		14.3	24.5	35.0	44.8	
	Avg	14.6	34.9	31.1	45.2	31.5
5	A	25.7	46.5	80.5	53.3	
		25.7	46.8	83.3	51.5	
		37.0	46.3	61.3	68.5	
	B	19.5	49.8	58.7	44.3	
		20.8	39.0	48.3	47.5	
		29.8	45.0	58.0	48.2	
	Avg	26.4	45.6	65.0	52.2	47.3
Within-texture avg		19.0	31.4	42.1	44.5	

Note: Each value is the average of six tests (two tests each by three technicians). Tests were performed at three different wheelpath locations for each test section and method combination.

Effects of Texturing Method

Figure 2 shows the effect of texturing method (based on average values for all five sites) on both initial mean texture depth and mean skid resistance at speeds of 40 and 55 mph. The fluted float and wire broom methods produced the deepest textures and the highest skid resistances. The results of statistical significance tests between pairs of these data are given in Table 7. The fluted float and wire broom methods produced virtually the same results.

Texture Depth Versus Initial Skid Resistance

The entrapment of water between a sliding tire and a wetted pavement surface is responsible for the development of hydrostatic pressure. Pavement-tire friction decreases as hydrostatic pressure increases. The low skid numbers attained at the testing speed of 55 mph (Fig. 2) reflect this principle. Similarly, the greater sensitivity of skid resistance to characteristics of the macrotexture at higher testing speeds is shown by the greater slope of the relationship at a speed of 55 mph (Fig. 2).

The primary pavement characteristic related to drainage is the mean hydraulic radius, i.e., the ratio of the cross-sectional area of the average drainage channel to its wetted perimeter (4). Because the wetted perimeter is so difficult to measure, Gillespie (5) worked with the drainage area alone and was able to show that it correlated with the skid characteristics of six actual pavements. Goodman (6) reasoned, therefore, that a measure of mean texture depth based on drainage area is equivalent to measuring the drainage area itself and cited "mean texture depth" derived from the sand-patch test as an example.

It is not surprising, therefore, to find the good correlations between texture depth and skid resistance shown in Figure 2. This is particularly true for the three conventional texturing methods, which all produce irregular patterns that vary primarily in depth. The fact that the texture produced by the fluted float method fits this same relationship suggests that its depth and drainage area are related to one another in the same way as in the textures produced by the other three methods. This suggestion is supported by the data shown in Figure 3. This figure shows the relationships between texture depth and drainage area and texture depth and skid resistance for one of the experimental sections. Drainage areas were measured from microprofiles by using a planimeter—a method similar to that used by Gillespie (5).

The relationship between skid resistance and texture depth in pavements, as measured by the the sand-patch test, has been demonstrated elsewhere (7, 8). This is the first time, however, to the authors' knowledge that the relationship has been shown to hold for a variety of textures produced in concrete by different methods. This tends to reinforce the significance of texture depth as a determinant of skid resistance.

Texture Depth Versus Coefficient-Speed Gradient

A paramater equally important as texture depth to skid resistance (as measured at a particular testing speed) is the rate at which skid resistance changes with testing speed—the so-called coefficient-speed gradient (9). The decrease in this gradient can be inferred from the convergence of the 40- and 55-mph lines with increasing texture depth as shown in Figures 2 and 4. The data shown in Figure 4 are based on average values of mean texture depth and coefficient-speed gradient for the 20-texture method and site combinations. The relationship is curvilinear—asymptotic on one end to a texture depth of 8 to 9 in. $\times 10^{-3}$ (representing no texture at all) and approaching zero gradient on the other as texture depth increases. This relationship has been demonstrated elsewhere (5, 10).

Uniformity of Texture Depth

Standard deviations of texture depth corresponding to each of the texturing methods are shown in Figure 5. Each standard deviation was computed from 30 values that represent mean texture depths measured at three points in the wheelpath of each of the 10 experimental sections. Figure 5 shows that, for the conventional texturing methods,

Table 5. Summary of initial skid numbers.

Site	Test Section	Initial Skid Number at 40 mph[a] Burlap Drag	Bristle Broom	Wire Broom	Fluted Float	Within-Site Avg	Initial Skid Number at 55 mph[a] Burlap Drag	Bristle Broom	Wire Broom	Fluted Float	Within-Site Avg
1	A	63	64	63	61		43	55	55	61	
		55	63	60	63		37	55	52	61	
	B	55	63	58	66		52	60	57	54	
		49	60	60	64		52	60	54	52	
	Avg	55.5	62.5	60.3	63.5	60.4	46.0	57.5	54.5	57.0	**53.8**
2	A	59	55	66	70		38	44	52	61	
		49	49	59	66		38	40	56	57	
	B	49	50	62	62		39	38	61	63	
		52	59	66	66		29	31	56	57	
	Avg	52.3	53.3	63.3	66.0	58.7	36.0	38.3	56.0	59.5	47.5
3	A	58	72	72	72		43	58	70	69	
		63	70	72	72		42	57	70	66	
	B	61	66	67	72		52	55	64	63	
		64	72	70	72		49	51	61	61	
	Avg	61.5	70.0	70.3	72.0	68.4	46.5	55.3	66.3	64.8	58.2
4	A	38	46	51	51		26	41	44	46	
		38	46	53	51		24	41	42	46	
	B	41	58	55	40		31	50	48	47	
		37	63	58	48		31	52	50	47	
	Avg	38.5	53.3	54.3	49.5	48.9	28.0	46.0	46.0	46.5	**41.6**
5	A	49	54	61	61		46	49	60	58	
		48	55	58	58		46	51	60	58	
	B	52	52	57	51		42	48	55	46	
		51	49	60	51		42	45	48	43	
	Avg	50.0	52.5	59.0	55.3	54.2	44.0	48.3	55.8	51.3	49.8
Within-method avg		51.6	58.3	61.4	61.3		40.1	49.1	55.8	55.8	

[a]Each value (except averages) represents one skid test.

Figure 2. Effect of texturing method on initial texture depth and skid resistance.

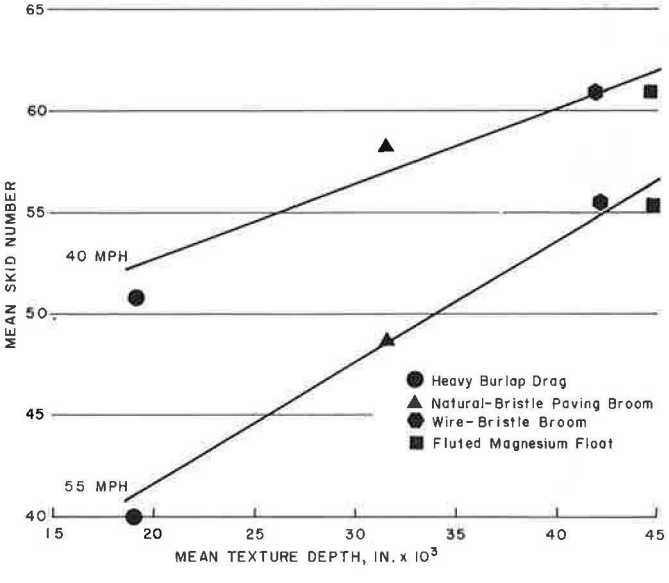

Table 6. Mean texture depth wear rates.

Site	Mean Texture Depth (in. x 10^3) Burlap Drag	Bristle Broom	Wire Broom	Fluted Float
1 (opened 7-70)				
Initial	24.9	32.1	45.2	**39.5**
9-70; 0.414 VP	20.9	25.7	37.0	**37.4**
4-71; 1.862 VP	8.5	10.0	16.5	**15.0**
8-71; 4.376 VP	8.0	9.2	15.0	**17.0**
2 (opened 10-69)	16.5	24.3	32.8	**48.6**
Initial	11.6	18.4	24.5	**43.7**
5-70; 2.880 VP	9.8	16.0	21.7	**40.4**
8-70; 4.323 VP	8.8	15.5	22.0	**40.9**
9-70; 4.320 VP	9.0	14.4	22.5	**39.2**
4-71; 6.840 VP				
3 (opened 12-70)				
Initial	12.4	20.0	36.4	**37.2**
5-71; 2.565 VP	8.0	9.7	19.3	**17.4**
8-71; 4.104 VP	8.0	9.2	18.7	**15.4**
4 (opened 8-70)				
Initial	14.6	34.9	31.1	**45.2**
9-70; 1.888 VP	9.8	22.7	21.7	**38.6**
5-71; 13.215 VP	8.0	10.5	11.5	**10.0**
8-71; 22.654 VP	8.0	8.2	8.9	**8.5**
5 (opened 12-70)				
Initial	26.4	45.6	65.0	**52.2**
3-71; 1.503 VP	15.4	19.7	31.5	**27.0**
8-71; 3.506 VP	8.3	15.8	27.0	**24.2**

Note: VP = estimated cumulative number of vehicle passes x 10^5; mean texture depth measured by using the sand patch method.

Table 7. Results of tests for significance of differences among texturing methods.

Texturing Methods Compared	Texture Depth	Skid Resistance At 40 mph	At 55 mph
Burlap drag			
Bristle broom	Significant	Significant	Significant
Wire broom	Significant	Significant	Significant
Fluted float	Significant	Significant	Significant
Bristle broom			
Wire broom	Significant	Not significant	Significant
Fluted float	Significant	Not significant	Significant
Wire broom			
Fluted float	Not significant	Not significant	Not significant

Note: Test conducted by using the student t-test at the 0.90 confidence level.

Figure 3. Relationships between texture depth and drainage area and texture depth and skid resistance, site 4, section B.

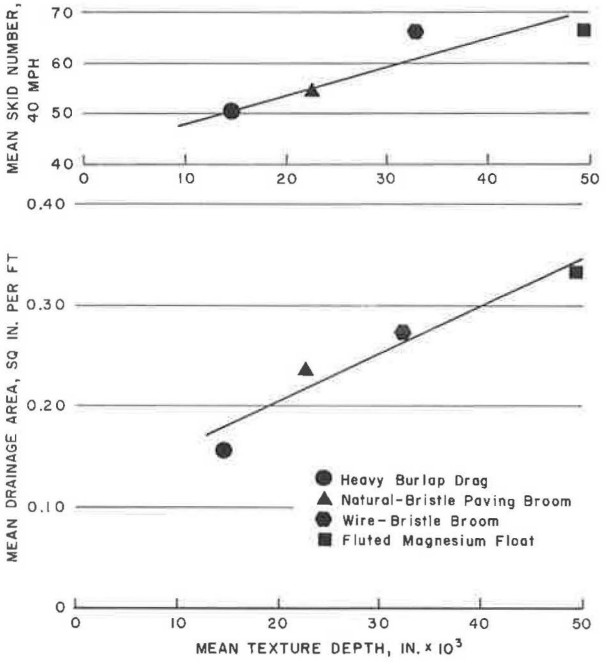

Figure 4. Effect of texture depth on coefficient-speed gradient.

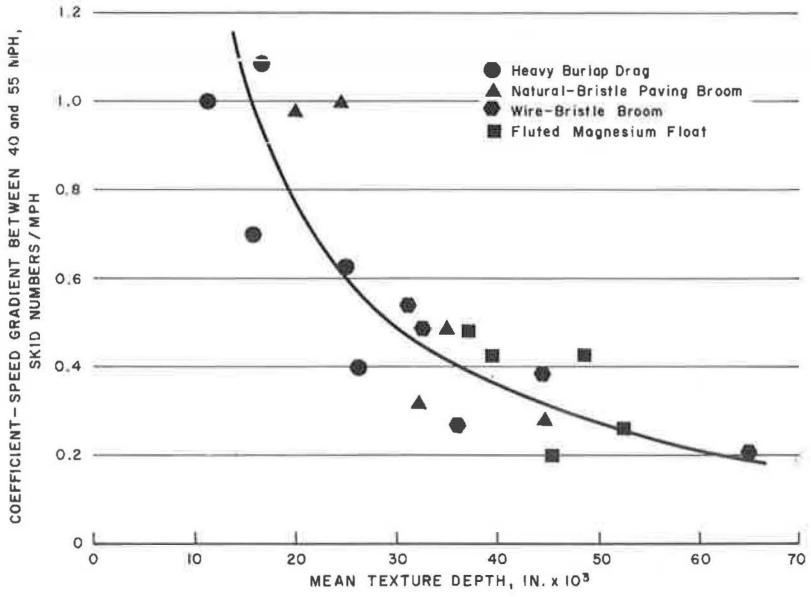

uniformity decreases with increasing mean texture depth. However, the texture produced by the fluted float method is one of the deepest, and its uniformity is relatively high. Apparently, this is because the fluted float (when manually operated) is less sensitive to variation in the stiffness of surface mortar at the time of texturing than are the other methods.

Durability of Texture and Skid Resistance

Because of the abrasion that results from increased traffic volume and speed, winter maintenance, and the use of tungsten carbide studs by a large portion of the driving public in New York State, even the deepest textures have little chance of surviving for more than a few years. At the most heavily traveled experimental location (site 4), for instance, all of the textures had been worn to mean depths of from 0.008 to 0.009 in. after the first year of service. This is equivalent to the complete removal of all macrotexture and corresponds to reductions in skid number of between 31 and 40 at a speed of 40 mph and 22 and 32 at a speed of 55 mph. From this experience, it could be argued that many high-volume, high-speed concrete highways may require maintenance to restore skid resistance long before they require it to level wheelpath ruts.

The range of decay in texture depth encountered in this study is shown in Figure 6. Sites 2 and 4 respectively show the least and the greatest wear after 1 year of service. Site 2 has the lowest driving-lane AADT and is snow-packed for 3½ months each year; thus, it does not receive nearly the volume of studded-tire traffic one would otherwise expect. Site 4 is a heavily traveled commuter route that is located outside of Rochester. It has the highest driving-lane AADT of the five sites.

The data shown in Figure 6 lead to the conclusion that the amount of pavement texture remaining at any particular time will depend primarily on the volume of traffic that has passed over it and on the texture's initial depth. Methods that produce deep textures, such as the wire-bristle broom and the fluted float, have an advantage in this respect.

If the texture wear data from site 2 are projected at the same decay rate and the traffic volume figures are corrected to account for the period of snowpack, the following generalization could be proposed:

> Under conditions where 35 to 40 percent of vehicle operators use studded tires for periods up to 6½ months of the year, a texture with an initial mean depth of 0.045 to 0.050 in. would be expected to last for 6 years or more if the AADT over the textured surface does not exceed 850. On the other hand, if the AADT over the surface exceeds 5,000, the texture would probably disappear in less than 1 year.

No consideration has been given in this discussion to the effect of the quality of the mortar in which the textures were actually placed on the rates of wear experienced. Although the importance of this factor is recognized, the authors believe that the durability of texture on a high-speed, high-volume highway such as that at site 4 depends primarily on total traffic volume.

The levels of skid resistance corresponding to texture depths at site 4 after 1 year of traffic have been noted. Figure 7 shows average depths and skid resistances, both initially (before opening to traffic) and in the summer of 1971, for textures at all experimental sites. As expected, the reduction in texture depth has been accompanied by a decay in skid resistance, and the textures have maintained the same order with respect to one another in both depth and skid resistance.

Texture Wear Rates

In an effort to look more closely at the effect that texturing methods have on the rate of texture wear, we computed average wear rates for the textures produced by each method after an average of only 200,000 vehicle passes. The results (Fig. 8) represent wear characteristics during the early service life of the textures. Two points are worth noting:

Figure 5. Effect of texturing method on uniformity of texture depth.

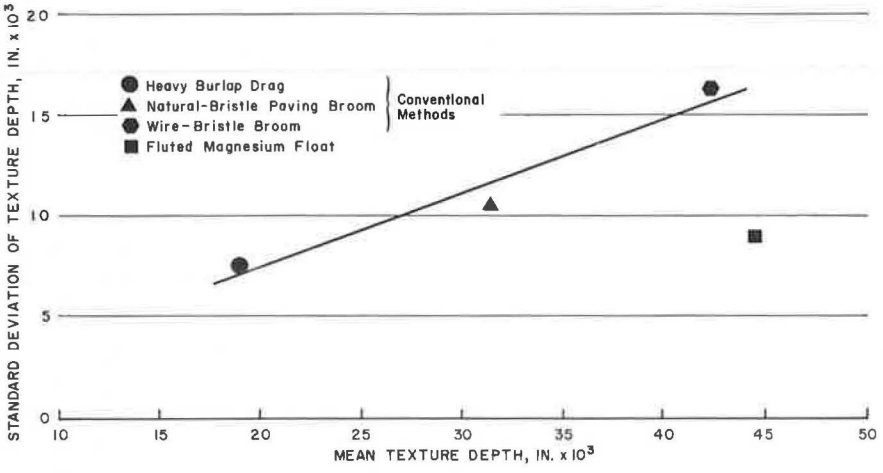

Figure 6. Decay of texture depth.

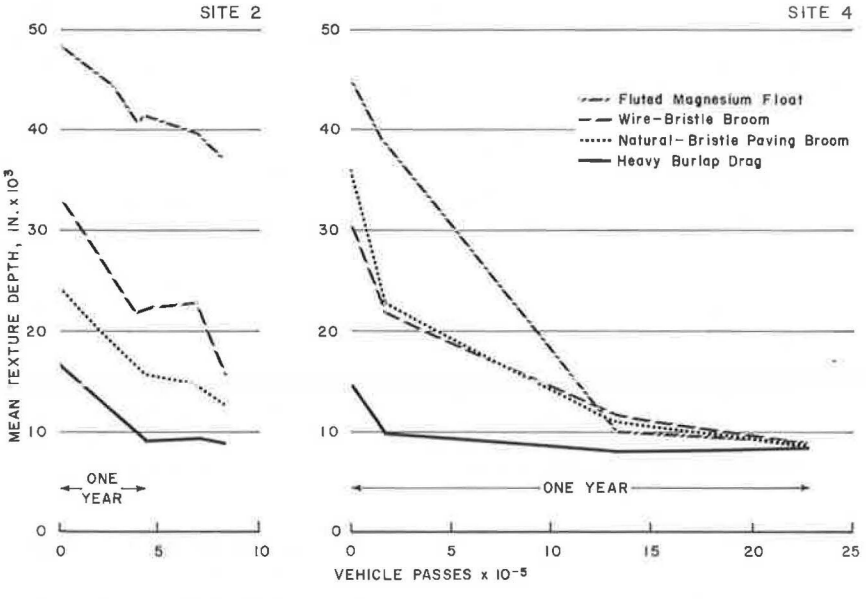

Figure 7. Changes in texture depth and skid resistance.

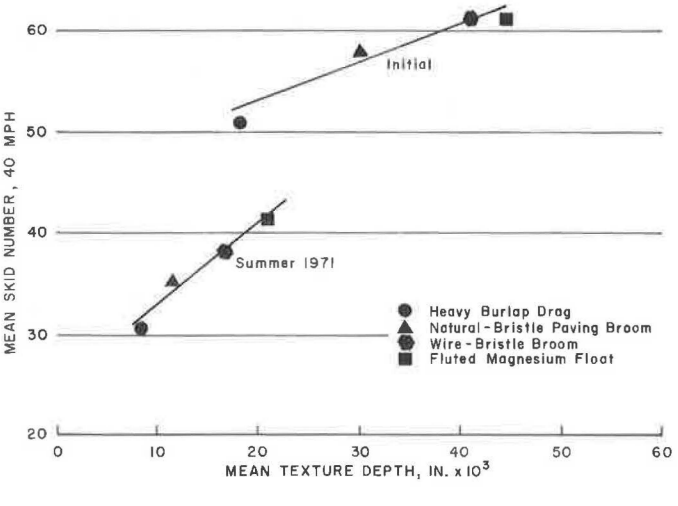

Figure 8. Early rates of texture wear.

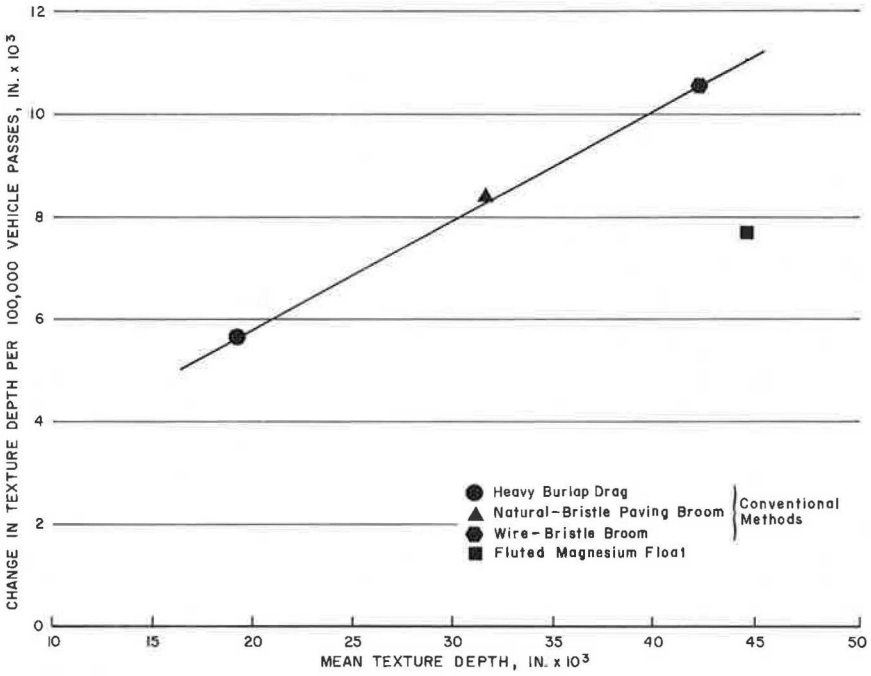

Figure 9. Hypothetical texture wear curve.

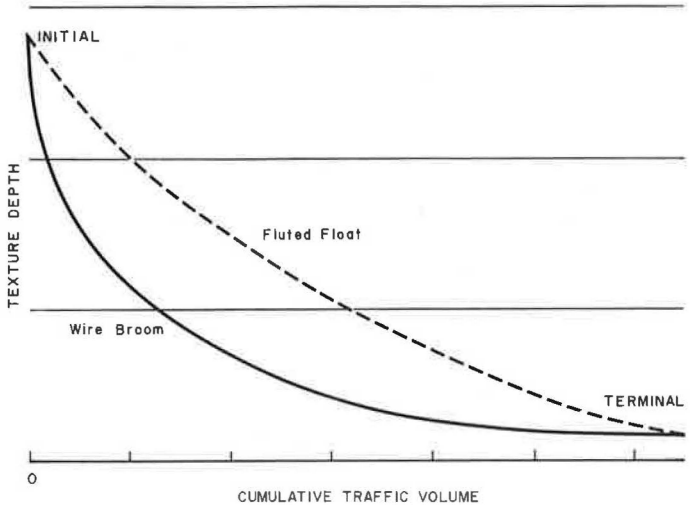

Table 8. Vehicle noise generated on study textures.

Texturing Method	Mean Texture Depth (in. x 10^3)	Sound Pressure Level[a] (dB)	
		At 50 mph	At 60 mph
Bristle broom	39	96.0	97.5
Wire broom	48	96.0	98.0
Fluted float	48	90.5	96.0

Note: Sound measured by using a sound level meter (Realistic Model No. 33-1028, operated in the "fast" response setting) with the 0 to 180 deg axis of the microphone perpendicular to the pavement edge.

[a]Reference 0.0002 μ bar.

1. As with uniformity, the early rate of wear appears to be a function of initial texture depth, at least for textures produced by the conventional methods; i.e., deeper textures wear faster. There may be two reasons for this. First, the deeper textures have higher "peaks" and "ridges," which are inherently more vulnerable to abrasion than are shallow textures because they carry higher unit loads than the pavement surface as a whole. Second, the rougher the texture is, the more vulnerable it may be to improper curing and abrasion. This would occur because of (a) the increased surface area and, therefore, thinner films for the same rate of membrane curing compound application; (b) the probable tendency for curing compounds to run off the "peaks" and collect in the "valleys"; and (c) the inaccessibility of certain surfaces to sprayed curing compounds.
2. In contrast to textures produced by the conventional methods, the relatively deep texture produced by the fluted float has an unexpectedly low rate of wear. This is probably because of the inherent abrasive resistance of its relatively smooth surface and the fact that it does not embody many of the features of more irregular surfaces that may inhibit proper curing.

It appears that the typical wear curve for any texture is one of decreasing negative slope (Fig. 6). Initially, the texture probably wears rapidly as the tips of the vulnerable peaks are abraded. With the passage of traffic, however, wear (decrease in texture depth) occurs at a progressively lower rate that corresponds to the increasingly larger surface available to carry tire loads. Textures produced by the fluted float method appear to have an advantage in this respect as well. Not only should the textures produced by the fluted float last longer because they are initially deeper than the textures produced by the other methods, but also they should wear at a more uniform rate and thus provide a greater average texture depth during their service life. The latter point is illustrated by Figure 9, which is a hypothetical wear curve for two textures having the same initial texture depth and life expectancy but different geometric configurations.

Sound Generation

Sound pressure level measurements were made of the passage of a 1968 Ford Fairlane passenger car, at cruising speed and with regular-tread tires, over three of the experimental textures at one of the sites. These measurements, summarized in Table 8, were made from a point 2 ft above ground and 2 ft outside the edge of pavement. No measures of spectral content of the sound were made. It appears from these limited observations that an increase in texture depth, within the range observed, is not associated with a significant increase in sound, as measured by sound pressure level. Also, for equivalent texture depths, the texture produced by the fluted float method may generate less sound than those produced by more conventional methods. No differences in sound pressure level were detectable from inside the automobile.

CONCLUSIONS

From the foregoing, the following specific conclusions can be drawn:

1. Textures produced by the different methods investigated varied significantly in both mean texture depth and initial skid resistance at speeds of 40 to 55 mph. Textures produced by the wire broom and fluted magnesium float methods were generally equivalent in mean texture depth and initial skid resistance and were superior to those produced by the natural-bristle broom and burlap drag methods.
2. Textures produced by the same method varied significantly from site to site in both mean texture depth and initial skid resistance.
3. Mean texture depth, as measured by the sand-patch method, correlated to a high degree with mean skid resistance for the variety of texturing methods studied both before and after exposure to traffic.
4. A high degree of correlation was also found between mean texture depth and the coefficient-speed gradient at speeds of 40 and 55 mph.
5. For the conventional texturing methods, uniformity of initial texture depth was found to vary inversely with mean texture depth. In contrast, the comparatively deep

texture produced by the fluted float method was nearly as uniform as that produced by the burlap drag method (the shallowest texture).

6. The amount of pavement texture remaining at any particular time varied considerably from site to site, depending primarily on cumulative traffic volume, initial texture depth, and wearing characteristics of the particular texture. With the 30 to 40 percent studded snow-tire use estimated for the experimental sites, the deepest textures were observed to last for less than 1 year under the heaviest traffic encountered and projected to last for 6 years under the lightest traffic.

7. The rate at which the textures produced at the same site by different methods were worn depended on initial texture depth and texturing method. Wear rate increased with increasing texture depth for the conventional texturing methods. In contrast, the texture produced by the unconventional fluted float method, which was one of the deepest, wore at a relatively moderate rate.

8. For equivalent texture depths, the texture produced by the fluted float method generated no more sound than did those produced by conventional methods.

SUMMARY

As a result of this work, fundamental and practical information has been obtained regarding the characteristics and performance of textures produced in concrete pavements by different methods. Because texture depth appears to be a reliable determinant of skid resistance, particularly at high speeds, it appears that the deeper the texture is, the safer the riding surface is. This, of course, must be consistent with considerations of tire wear, noise generation, and riding quality. Noise generation and riding quality do not seem to be problems within the range of texture depths now under consideration.

There appear to be some disadvantages in using deep textures, at least those produced by methods that might be considered conventional. It may be more difficult, for instance, to control the uniformity of deep textures. Of greater significance, though, is the tendency of deep textures to wear more rapidly during their early service life, which would rapidly nullify their initial advantage.

One possible route to producing an optimum texture is to design its geometry as other components of the highway are designed. Some possibilities are suggested by the performance of the texture produced by the fluted float method. This method not only provided deep textures with high skid resistance and low coefficient-speed gradients, but it also produced textures that were more uniform and that appeared to wear at a lower rate. The texture produced by this method rides well and may generate less noise than textures of equal mean depth that are placed by other methods. Further study of the parameters of texture geometry and how they relate to the characteristics of texture performance is suggested.

If, as is widely accepted, studded tires are responsible for accelerated pavement wear, many of the considerations discussed here are probably largely academic, at least in those regions of the country where studded tires have attained a substantial degree of public acceptance. The most compelling argument against the use of studded tires may not be rutting, hydroplaning, or the ultimate repair bill, but the drastic reduction of skid resistance that may be occurring on many new, high-speed, high-volume concrete highways as the result of accelerated wear of textures.

ACKNOWLEDGMENTS

Use of the fluted magnesium float to texture concrete pavements was suggested originally by Bernard M. Evans and Philip A. Barnes of the New York State Department of Transportation. Data were collected under the supervision of Donald G. Riccio, with the assistance of Edward F. Gremmler, Jr., and Thomas F. VanBramer. Michael W. Fitzpatrick and John VanZweden were responsible for measuring the skid resistance of experimental pavements.

REFERENCES

1. Kummer, H. W., and Meyer, W. E. Tentative Skid-Resistance Requirements for Main Rural Highways. NCHRP Rept. 37, 1967, 80 pp.
2. Instructions for Using the Portable Skid-Resistance Tester. Road Research Laboratory, Note 27, 1960.
3. Duncan, A. J. Quality Control and Industrial Statistics. Richard D. Irwin, Inc., Homewood, Ill., 1965, pp. 503-504.
4. Moore, D. T. The Measurement of Surface Texture and Drainage Capacity of Pavements. Proc., 1968 International Colloquium on the Interrelation of Skidding Resistance and Traffic Safety on Wet Roads, Verlag von Wilhelm Ernst und Sohn, Berlin, Vol. 2, 1970, pp. 537-551.
5. Gillespie, T. D. Pavement Surface Characteristics and Their Correlation With Skid Resistance. Pennsylvania Department of Highways and Pennsylvania State University, Joint Road Friction Program, Report 12, 1965.
6. Goodman, H. A. Pavement Texture Measurement From a Moving Vehicle. Pennsylvania Department of Highways and Pennsylvania State University, Joint Road Friction Program, Report 19, 1970.
7. Sabey, B. E. Road Surface Texture and the Change in Skidding Resistance With Speed. Road Research Laboratory, RRL Rept. 20, 1966.
8. Pasquet, A. The 1967 National Slipperiness Campaign in France—Main Results of Measurements of Skidding Resistance. Proc., 1968 International Colloquium on the Interrelation of Skidding Resistance and Traffic Safety on Wet Roads, Verlag von Wilhelm Ernst und Sohn, Berlin, Vol. 2, 1970, pp. 717-731.
9. Schulze, K. H., and Beckman, L. Friction Properties of Pavement at Different Speeds. ASTM Spec. Tech. Rept. 326, 1962, pp. 42-49.
10. Sabey, B. E. Road Surface Characteristics and Skidding Resistance. British Granite and Whinstone Association Journal, Vol. 5, No. 2, Autumn 1965, pp. 7-18.

APPENDIX

DETAILS OF EXPERIMENTAL TEXTURING DEVICES

Burlap Drag

The burlap drag consists of four layers of 10.4-oz burlap that are 5 ft long and 4 ft wide. The device is used in a damp state.

Natural-Bristle Broom

The natural-bristle broom has a 3.7-lb broom head consisting of a 16-in. long by 4-in. wide by 2-in. deep wooden block with 6-in. long, 100-bristle tufts in five rows on $\frac{3}{4}$-in. centers; individual bristles are $\frac{1}{32}$ to $\frac{1}{8}$ in. wide and approximately $\frac{1}{32}$ in. thick.

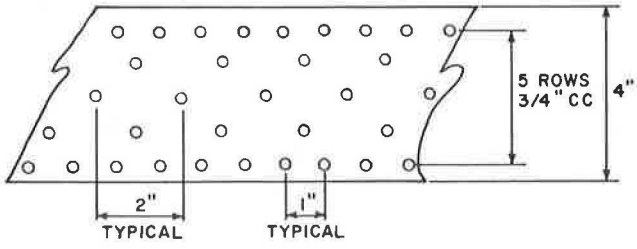

Wire-Bristle Broom

The wire-bristle broom has a 4.5-lb broom head consisting of a 28-in. long by 3-in. wide by 2-in. deep wooden block with 5-in. long, 10-bristle tufts in two rows on $\frac{7}{8}$-in.

centers; individual bristles consist of $^{1}/_{16}$- by $^{1}/_{100}$-in. steel tapes.

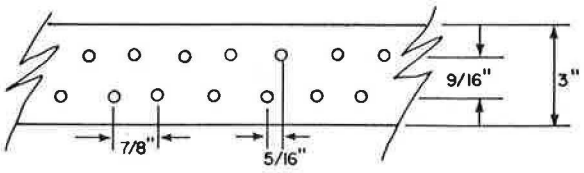

Fluted Magnesium Float

The fluted magnesium float has a 10.4-lb float head 40 in. long and $7^{1}/_{2}$ in. wide, which is fluted to produce a nominal pattern.

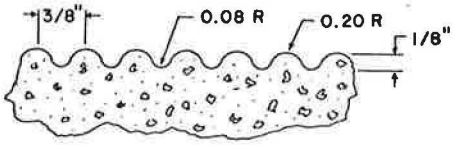

CONSTRUCTION OF A PREFABRICATED HIGHWAY TEST SECTION

Lorys J. Larson, South Dakota State University; and
Wayne R. Haug, State Highway Commission of Kansas

A unique section of highway is being tested under regular traffic conditions on the US-14 bypass near Brookings, South Dakota. It consists of a 900-ft stretch of two-lane highway constructed of precast, prestressed concrete panels 6 ft wide, 24 ft long, and 4½ in. thick. The panels are overlaid with a bituminous mat that ranges in thickness from 3 in. at the centerline to 1½ in. at the edges. The prefabricated panels are designed to replace conventional pavement more than 10 in. thick that may be required for the heavier loads of the future. Evaluation of structural performance is continuing and will be made available at a later date. This paper is a brief account of the procedures utilized in the construction of this test section. A cost summary is also included showing that this type of pavement costs about $15 per sq yd. The cost is not competitive with current conventional pavements. However, the precast, prestressed concrete panel concept was visualized as a possible solution for future highway loads that may require increased thickness for conventional pavements. At that time, this type of prefabricated highway could become economically feasible.

•BECAUSE of the increase in heavy-truck traffic, stronger pavements are needed to carry the increasing wheel loads. This has resulted in the development of thicker pavements that cost more. In some parts of the country the aggregates needed for such pavements are scarce, which makes it necessary to transport the aggregates over long distances to the construction site. Long haul transportation increases the pavement cost further; therefore, it is necessary to investigate other methods of construction.

During the past three decades, research has resulted in the development of prestressed concrete pavements that are composed of concrete prestressed with high-strength steel (1, 2, 3, 4, 5, 6). As a result of prestressing, both the high compressive strength of the concrete and the high tensile strength of the steel are utilized. Through utilization of the compressive strength, the prestressed concrete slab can be thinner yet have the same load-carrying capability as ordinary concrete pavement. Such a reduction in thickness means a saving in aggregate as well as a possible saving in construction time. As the size of vehicle loads increases, the use of prestressed concrete pavements should become economically competitive with current methods of construction.

In 1962, the Civil Engineering Department at South Dakota State University, in cooperation with the South Dakota Department of Highways and the U.S. Department of Transportation, Federal Highway Administration, initiated a study to determine the suitability of precast, prestressed concrete panels for use in highway pavements.

In 1962, Gorsuch (7) constructed a laboratory test to determine the structural behavior of precast, prestressed concrete panels. He used half-scale test panels 12 ft long, 2 ft wide, and 2 in. thick. The panels were laid in a transverse direction and were post-tensioned in the logitudinal direction. From a structural standpoint, the panel sections held promise for use in highway pavements.

Further laboratory testing was made by Kruse (8) in 1966 to evaluate the feasibility of using prestressed and post-tensioned concrete panels and to make recommendations for possible field studies. The test panels were each 24 ft long, 4 ft wide, and 4½ in.

Sponsored by Committee on Rigid Pavement Construction.

thick. These panels were pretensioned in the longitudinal direction by five steel cables, each of which was $^3/_8$ in. in diameter. Each cable consisted of 7-wire steel strands. The panels were also post-tensioned in the transverse direction. A repetitive wheel loading was used. This study showed that the pavement ($4^1/_2$ in. thick) was structurally adequate for heavy-duty highway service and that pumping of the subgrade was a principal factor. Kruse suggested that further laboratory studies be made with heavier loads under adverse conditions that would be conducive to subgrade pumping. The suggested field studies included the testing of the precast panels, direction of pretensioning, expansion joints, distance between joints, total panel movement, subgrade friction, and the investigation of methods by which the panels are transported and handled.

In 1967, a study was conducted by Jacoby (9) dealing with thermal expansion and contraction in a pavement consisting of prestressed concrete panels. This study was divided into a laboratory study and a small-scale field test section. Half-scale panels were used in the laboratory study, whereas full-scale panels were used in the field study. The field study panels were 24 ft long, 6 ft wide, and $4^1/_2$ in. thick. Nine 7-wire steel strands ($^3/_8$ in. in diameter each) were used to develop a prestress of 350 psi in the longitudinal direction. No prestress was used in the transverse direction. The 96- by 24-ft field test section was located near the South Dakota Department of Highways' maintenance yards near Brookings, South Dakota. It was subjected to highway department vehicles moving at speeds of less than 25 mph.

The findings of the studies at South Dakota State University have resulted in the continued study of a special test section constructed with prestressed concrete pavement panels overlaid with asphalt concrete and located on the US-14 bypass north of Brookings, South Dakota, adjacent to South Dakota State University.

The present paper is a brief account of the construction procedures and costs involved in the construction of the precast, prestressed composite pavement test section now in public use near Brookings, South Dakota. Research now in progress involves a 5-year study of the cost and performance of this pavement under actual traffic conditions. The study began in 1967 for the South Dakota Department of Highways in cooperation with the U.S. Department of Transportation, Federal Highway Administration.

PANEL ARRANGEMENT AND CONFIGURATION

The 900-ft long by 24-ft wide test section was divided into two parts. In the east part of the test section (504 ft), the panels were laid in the longitudinal direction; in the west part (396 ft), the panels were place in the transverse direction (Fig. 1).

After consideration of design loadings and lifting stresses, it was found that lifting and handling stresses were critical. Accordingly, all panels were designed to accommodate the stresses while holding the panel thickness to the considered minimum of $4^1/_2$ in.

Four steel loops were precast into the panels for lifting and handling. For each panel, the loops were located 5 ft from each end and 1 ft from the side. The stresses, which resulted 5 ft from each end due to lifting, were 612 psi of compression at the top of the panels and 196 psi of compression at the bottom.

The panels were constructed at Gage Brothers Concrete Company in Sioux Falls, South Dakota. All panels were 24 ft long, 6 ft wide, and $4^1/_2$ in. thick with the exception of 4 end panels that were 12 ft long, 6 ft wide, and $4^1/_2$ in. thick. A uniform prestress of 405 psi was obtained in the longitudinal direction by using ten $^3/_8$ in. diameter, 7-wire steel strands, high-strength steel cables having a yield stress of 270,000 psi. The panels were all reinforced in the transverse direction with No. 3 reinforcing bars spaced at 1-ft centers (Fig. 2).

Tapered grout keyways were constructed on all adjoining sides of the panels. These were subsequently filled with portland cement mortar grout to provide a shear transfer from one panel to another (Fig. 3).

For the east portion of the test section, the panels were constructed with protruding reinforcing bars that provided for a welded connection (primarily for holding the panels in place during construction) at a distance of 6 ft from the panel ends. At these points, access for welding was furnished by widening the grout keyway 2 in. for a distance of 4 in. (Fig. 3).

Figure 1. Test section plan.

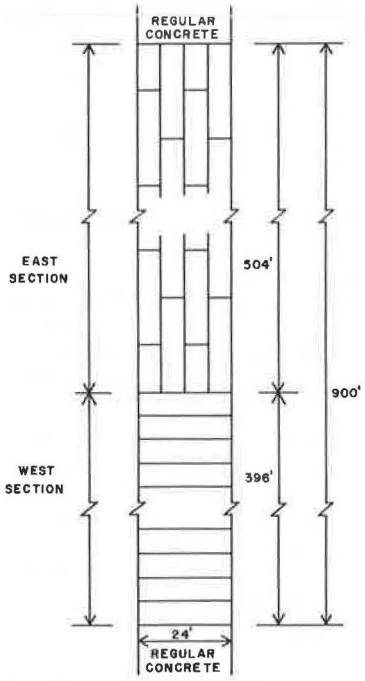

Figure 2. Typical panel details.

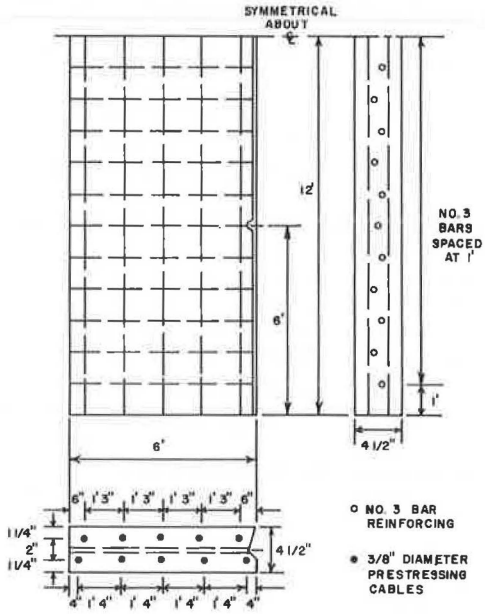

Figure 3. Grout key and connection joint sections.

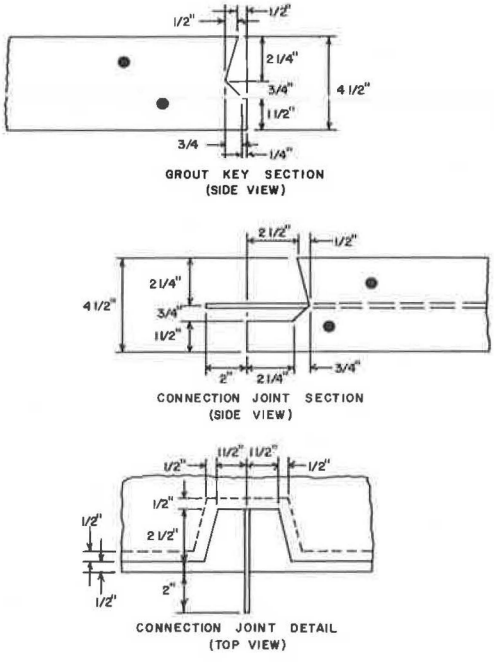

The panels for the west portion of the test section were designed without the welded connections between the panels.

SUBGRADE PREPARATION

The subgrade was constructed by undercutting through cut sections and shallow fill sections, 3 ft below the proposed earth subgrade, to ensure that there was a minimum fill height of 3 ft. The subgrade embankment was compacted to 8- to 10-in. lifts to meet specified moisture and density criteria by using sandy silt fill material from a nearby borrow pit. Crushed gravel subbase was then added and compacted to produce the necessary transverse slope and thickness, with a 3-in. minimum thickness provided at the centerline after fine grading.

An autograder was used to fine grade the base course to the correct elevation. The base course and subbase were then compacted with a pneumatic self-propelled roller, and the paver track forms were installed at the correct elevation.

Prior to placing the precast panels, a $\frac{1}{2}$-in. layer of bedding sand was added. A tail blade, operating on track forms, leveled the bedding sand and established the correct elevation.

A typical cross section of the finished pavement is shown in Figure 4.

PLACEMENT OF PANELS

The panels, which had been transported to the construction site by trucks, were unloaded on the shoulder of the road by a hydraulic crane. The panels were lifted by using the four steel loops that were precast into each panel. Before the panels were laid in place on the highway, a bond breaker (RC 250 asphalt) was applied along one edge of the panels to prevent the grout (placed in the joints later) from bonding along one edge of the keyway.

The placement of the panels began at the east end of the site, where they were placed in the longitudinal direction (Fig. 5). The track forms were utilized for alignment. The panels were later connected by welding together the steel reinforcing bars provided at each connection point.

The panels in the west section of the test site were placed in the transverse direction (Fig. 6). These panels were not provided with welded connections.

After the panels had been placed on the base course, the steel loops, which were used in handling, were burned off with an acetylene torch. Wooden planks were then placed on the in-place panels, and a vibrator type of roller was used to ensure that the panels were firmly placed in the bedding sand.

Initially, the contractor attempted to use an air-pressure grout machine to fill the grout keyways; however, this machine proved inadequate, and a piston-driven grout machine was used to complete the grouting operation. Immediately after the grouting had been completed, the panel assembly was covered with polyethylene for curing.

A tack coat of RC 70 asphalt was applied prior to covering the panels with a Class G asphaltic concrete mat. Mat thickness ranged from 3 in. at the center of the roadway to $1\frac{1}{2}$ in. at the edges. The mat provided a crown for the highway as well as a smooth riding surface.

A summary of equipment, labor, and material costs of the test section is given in Table 1.

CONVENTIONAL CONCRETE PAVEMENT COSTS

Current construction costs of conventional pavements were obtained from several states within the same geographical area (Table 2). These states were chosen because they had similar climatic and terrain features. Construction methods and practices were about the same throughout the area. The costs cited are averages and refer to portland cement concrete pavements 24 ft wide. The cost per square yard varied from $5.21 for nonreinforced pavement to $7.89 for continuously reinforced pavement. The cost of earthwork, subgrade, or base construction is not included because it does not vary with type of pavement used.

Figure 4. Fine grading the subbase.

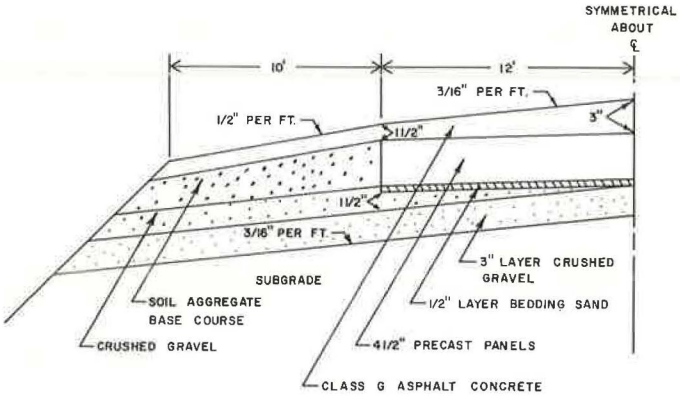

Figure 5. Placing panels in the east section.

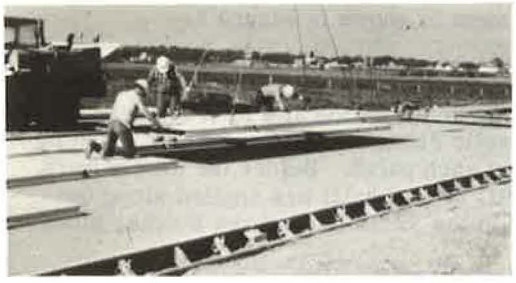

Figure 6. Placing panels in the west section.

Table 1. Test section costs.

Item	Equipment Rental (dollars)	Equipment[a] (dollars)	Equipment Total (dollars)	Labor (dollars)	Material (dollars)	Total (dollars)	Total Cost Per Square Yard (dollars)
Precast panels	—	—	—	—	32,698.00	32,698.00	13.62
Transportation	1,262.13	412.60	1,674.73	305.73	—	1,980.49	0.83
Unloading panels	324.68	244.23	568.91	132.44	—	701.32	0.29
Fine grading subbase	414.60	—	414.60	167.63	—	582.23	0.24
Bedding sand	552.91	64.35	617.26	326.35	126.90	1,070.51	0.45
Placing panels	752.82	186.83	939.65	534.62	—	1,476.27	0.62
Grouting panels	2,940.29	238.96	3,179.25	536.84	343.35	4,059.44	1.69
Asphalt mat	—	—	—	—	2,232.24	2,230.24	0.93
Total	6,247.43	1,146.97	7,394.40	2,003.61	35,400.49	44,798.50	18.67

[a]Equipment on project but not in use.

Table 2. Conventional concrete pavement costs.

State	Year	Type of Reinforcement	Pavement Thickness (in.)	Cost Per Square Yard (dollars)
South Dakota	1968	Nonreinforced	8	6.50
North Dakota	1966	Continuously reinforced	7	6.65
North Dakota	1967	Continuously reinforced	8	6.55
Wyoming	1968	Nonreinforced	8	5.53
Minnesota	1968	Reinforced	9	6.30
Iowa	1968	Nonreinforced	8	5.21
Iowa	1968	Reinforced	10	7.89
Iowa	1968	Continuously reinforced	8	7.20

CONSTRUCTION PROCEDURES AND COSTS

The 1967-1968 cost of the precast, prestressed concrete pavement is considerably higher than that listed for conventional pavement construction. However, it is believed that the $18.67 per sq yd cost of the prefabricated test section can be appreciably reduced. Mass production and familiarity with this type of highway construction would materially reduce overall construction costs. Because this is a new type of construction, considerable time was spent by personnel in learning the technique of placing the panels. Similarly, the cost of unloading the panels at the site could be reduced if an experienced crew were used to move the panels directly from the trucks to their placement on the highway. This would eliminate dual handling.

Costly experimentation with two types of grouting machines resulted in unnecessary expense to the contractor. Proper planning and experience with this type of operation could reduce grouting equipment costs by as much as $1.00 per sq yd.

The contractor made excellent use of the paver track forms to reduce the time and cost of construction. The forms were used by the tail blade to smooth the bedding sand and to obtain the correct elevation after the base course had been fine graded with the autograder. The forms also served to confine the bedding sand, and they were used as alignment guides during placement operations.

The panels could be produced at central casting yards on a year-round basis with quality control, which would provide concrete of high durability. The precast panels could then be trucked to places having weather conditions that might not be suitable for conventional pavement construction. This flexibility could have the same effect as lengthening the construction season.

The asphalt mat provides a smooth riding surface as well as a protective covering over the concrete panels and joints. Reflection cracking prevails over the panel joints during the winter months; however, these tend to seal themselves with the advent of warmer weather.

If a section of this pavement needs repair, the panels can be removed and replaced with new panels in a short period of time, thus lowering maintenance costs.

Conventional pavements are being constructed with greater thicknesses to carry the increasing loads required of current highways. Thus, greater quantities of high-quality aggregates are required. As a result, good aggregates are becoming scarce, and their price continues to rise, which makes conventional pavements increasingly more expensive.

It is felt that the total cost of this pavement could be reduced to somewhat less than $15.00 per sq yd. This figure is still not competitive with the current price of conventional 7- to 10-in. thick pavements. However, the type of pavement under consideration was visualized for use with heavy loads of the future that may require conventional pavements of 15 in. or more in thickness. Under these requirements, the precast panels would become economically competitive.

In addition to highway pavement use, precast, prestressed concrete panels could be stockpiled and used in the construction of parking lots and driveways. The U.S. Corps of Engineers has also expressed interest in the use of this type of panel for boat landing ramps.

CONCLUSIONS

This investigation to date has produced the following conclusions:

1. With increased expreience and the development of new construction techniques, the cost per unit area for precast, prestressed concrete composite pavement could be reduced to a price somewhat below $15.00 per sq yd.
2. The use of central casting yards would result in quality production in fabricating the concrete panels.
3. Precast, prestressed concrete panels could be placed during weather conditions that are not conducive to the placing of conventional pavements, thus lengthening the construction season.
4. As aggregates become more scarce, the precast panel system should become more competitive with conventional pavements.

5. As the thicknesses of conventional pavements increase because of heavier loads in the future, this type of precast panel construction would become more feasible.
6. Precast panels could be used for construction of parking lots, driveways, and boat landing ramps.
7. Subject to structural performance, precast, prestressed concrete composite pavement suggests a possible solution for future highway construction.

ACKNOWLEDGMENTS

The authors wish to express their appreciation to the South Dakota Department of Highways and the U.S. Department of Transportation, Federal Highway Administration, for their cooperation and assistance in this study. The opinions, findings, and conclusions expressed in this paper are those of the authors and not necessarily those of the Federal Highway Administration or of the South Dakota Department of Highways.

REFERENCES

1. LaLande, M. The Variety of Applications of Prestressed Concrete. Cement and and Concrete Association, 52 Grosvenor Gardens, London, 1949.
2. Friberg, B. F. Pavement Research, Design, and Prestressed Concrete. HRB Proc., Vol. 34, 1955, pp. 65-84.
3. Moreell, B., Murray, J. J., and Heinzerling, J. E. Experimental Prestressed Concrete Highway Project in Pittsburgh. HRB Proc., Vol. 37, 1958, pp. 150-193.
4. Vandepitte, D. Prestressed Concrete Pavements—A Review of European Practice. Prestressed Concrete Institute Journal, Vol. 6-7, March 1961, pp. 60-74.
5. Freibauer, B. Pretensioned Prestressed Concrete Slabs for the Vienna Airport. Prestressed Concrete Institute Journal, Vol. 6-7, March 1961, pp. 48-59.
6. Renz, C. F., and Melville, P. L. Experience With Prestressed Concrete Airfield Pavements in the U.S. Prestressed Concrete Institute Journal, Vol. 6-7, March 1961, pp. 75-92.
7. Gorsuch, R. F. Preliminary Investigation of Precast Prestressed Concrete Pavement. MS thesis, South Dakota State University, 1962.
8. Kruse, C. G. A Laboratory Analysis of a Composite Pavement Consisting of Prestressed and Post-Tensioned Concrete Panels Covered With Asphaltic Concrete. MS thesis, South Dakota State University, 1966.
9. Jacoby, G. A. A Study of Expansion and Contraction in a Pavement Consisting of Prestressed Concrete Panels Interconnected in Place. MS thesis, South Dakota State University, 1967.

LONGEVITY OF HOT-POURED ELASTOMERIC JOINT SEALANTS

Frank D. Gaus, Superior Products Company

•TWENTY years ago, Federal Specification SS-S-164 (AASHO M-173) was issued for a hot-poured joint sealing compound. It stated that the compound should be "a mixture of materials which will form a resilient and adhesive compound capable of effectively sealing joints in concrete against the infiltration of moisture throughout repeated cycles of expansion and contraction and which will not flow from the joints or be picked up by vehicle tires at summer temperatures." According to figures issued by the Federal Highway Administration in September 1970, 42 state highway departments still use a sealing compound that meets the requirements of this specification.

In 1968, an up-dated specification was issued by the United States Air Force as Federal Specification SS-S-1401A. The major changes included in this specification were a resiliency requirement and a requirement for a longer cooking period of material prior to its preparation for testing. It did not include tests for longevity or resistance to weathering.

There has long been a need for an improved hot-poured sealing compound. This topic has been discussed frequently at many national and international symposia (1, 2, 3, 4, 5). In response to this need, we have developed a polyvinyl chloride (PVC) hot-poured elastomeric sealant that will give long-term performance.

THE RESISTANCE OF HOT-POURED SEALANTS TO WEATHERING

During the early stages of PVC sealant development in 1963, tests were conducted on a newly developed PVC elastomeric hot-poured sealant by using a Weather-Ometer. The artificial-weathering test method contained in Interim Federal Specification SS-S-00200c for polysulfide-coal tar extended sealants was used to compare weathering properties. We learned that the PVC sealant was much more resistant to weathering than was the polysulfide-coal tar sealant.

During the past 8 years, our consultants have purchased various types of hot-poured sealants and have tested every hot-poured sealant that conforms to Federal Specifications SS-S-164, SS-S-167b, and SS-S-1401A, AASHO M-173, and the so-called Minnesota up-graded type. The materials were tested for resistance to weathering and flow characteristics by using the artificial-weathering test method. The testing program disclosed that certain hot-poured sealing compounds start to blister and bubble after just 1 hour; the SS-S-00200c specification requires that the full test be run for 160 hours. When it was learned that the 1401A sealing compound used in 1968 had very poor resistance to artificial weathering, we initiated a program to correlate laboratory artificial-weathering test results with field installation results. The 1401A materials and the PVC sealants that were installed in 1963 were compared.

Cook (6) was absolutely correct when he stated, in reference to the new 1401A, "The 164 specification had, for years, been the standard specification. The 1401 specification is a recent amendment. The addition of the resiliency requirement forces the manufacturer to upgrade the rubber content of the material. The materials which meet this newer specification look good, but require long-term field verification."

Sponsored by Committee on Sealants and Fillers for Joints and Cracks.

Artificial-weathering test panels were used at various installations such as the Kansas City International Airport and military air bases and were tested by the highway departments of Minnesota, Louisiana, Texas, and California. All of these participants reported that the materials eventually oxidized, bubbled, blistered, hardened, and flowed or pumped out of the joint, as had been predicted by the laboratory artificial-weathering tests. The findings of the program are reported in detail elsewhere (4).

At the same time, the PVC installations showed no signs of blistering, bubbling, cohesive failure, adhesive failure, or hardening after 9 years in areas subject to all types of weather conditions such as Detroit, Michigan; northern and southern California; Nevada; and Texas.

The positive correlation between the results of the field study and the artificial-weathering research in the laboratory is the basis for the development of a new specification for a hot-poured sealant for highways and airfields. This sealant will satisfactorily seal a joint watertight, resist intrusion of dirt and aggregate by maintaining resiliency, without adhesive or cohesive failure or blistering, bubbling, or hardening, for a period of from 15 to 20 years.

Field surveys of sealants over the past 4 years indicate that long-term performance is being obtained by using preformed neoprene compression seals in new construction, provided a premium adhesive-lubricant is used to place and hold the seal in the joint. A recent report based on 22 years of investigation by the state of Michigan (7) indicates that the neoprene compression seal loses as much as 70 percent of its initial compression in only 2 years, which substantiates that a premium adhesive-lubricant is mandatory for long-term seal performance. PVC hot-poured elastomeric sealants are providing the same long-term performance in new construction as well as in maintenance work.

RESEALING MAINTENANCE OF JOINTS

It is evident that funds for the maintenance of joints are becoming more and more scarce. Because of the increase in traffic volume, more and more of the maintenance dollar is being spent on "traffic control."

The increase in population and traffic makes it mandatory that a long-lasting sealant be used initially, whether it is a premolded neoprene compression seal or a PVC hot-poured elastomeric sealant, in new construction in concrete pavement. This type of sealant should also be used in resealing existing highway joints.

Rissel (8) points out that labor costs are rising faster than any other aspect of maintenance work, and he concludes that the best material should be used in the resealing of joints.

PVC elastomeric hot-poured sealants can be used for resealing highway joints and can provide long-term performance. The cleaning operation is fast: A plow can be used to remove old material; diamond concrete saw blades can be run through the joint to clean and shape it; the joint can be cleaned by a fast, thorough sandblasting; and then the sealant can be applied rapidly to the joint. Traffic may be opened immediately after the sealant has cooled in the joint. The sealant is applied at the low temperature of 250 F to 280 F. This low temperature does not deteriorate the polymer ingredient of the sealant.

For new construction or resealing of joints, the joint shape factor is an accepted and proven fact. The joint should be 1¼ in. in depth with the sealant applied to ¼ in. below the pavement surface.

A nonproprietary performance specification is available for the highway PVC elastomeric polymer hot-poured sealant and for the JFR type for use in critical areas of airfield pavements subject to jet fuel spillage and jet blast[1].

[1] The original manuscript of this paper included an appendix, Specification for Sealing Compound Elastomeric, Polymer-Type, Hot-Applied One Component, for Portland Cement Concrete Pavements. The appendix is available in Xerox form at cost of reproduction and handling from the Highway Research Board. When ordering, refer to Xerox Supplement 40, Highway Research Record 389.

The general requirements of the performance specifications state,

> The sealing compound when in place shall form a resilient and adhesive compound which is highly resistant to weathering, shall effectively seal joints in concrete against the infiltration of moisture throughout repeated cycles of expansion and contraction, and shall not flow from the joint or be picked up by vehicle tires at an ambient temperature of 70 F with full impact of solar radiation. The sealing compound before placement shall be stable at the safe heating temperature for up to three hours. The filled joints shall be free of large internal voids due to placement or voids which develop subsequently in service.

REFERENCES

1. Internat. Symposium on Joint Movement, Design, and Material. Brighton, England, May 1970.
2. Cook, J. P., and Lewis, R. M. Evaluation of Pavement Joint and Crack Sealing Materials and Practices. NCHRP Rept. 38, 1967, 40 pp.
3. McGhee, K. H., and McElroy, B. B. Study of Sealing Practices for Rigid Pavement Joints. Virginia Highway Research Council, June 1971.
4. Gaus, F. D. New Developments in Upgraded Hot-Poured Liquid Sealants. Proc., Symposium on Portland Cement Concrete Paving Joints, U. S. Department of Transportation, Wash., D. C., Sept. 22-23, 1970.
5. American Concrete Institute Committee 504, Guide to Joint Sealants for Concrete Structures. ACI Jour., Vol. 67, No. 67031, July 1970, pp. 489-536.
6. Cook, J. P. Construction Sealants and Adhesives. John Wiley and Sons, 1970.
7. Oehler, L. T., and Bashore, F. J. Michigan's Experience With Neoprene Compression Seal. Proc., 1971 Symposium on Joint Sealants, American Concrete Institute Committee 504, Denver, March 1971.
8. Rissel, M. C. Maintenance Equipment Training Programs for Operators and Mechanics. AASHO Proc., Oct. 1969.

EFFECTS OF VARIOUS SEALING SYSTEMS ON PORTLAND CEMENT CONCRETE JOINTS

Delmont D. Brown, The D. S. Brown Company, North Baltimore, Ohio

•NEOPRENE compression seals are becoming recognized as the most effective means of sealing expansion and contraction joints in concrete pavements, bridges, and other projects where joints are needed for the expansion and contraction of the structural mass. The question has arisen of whether the use of compression seals actually increases the life of the joints with a corresponding increase in the life of the structure. The purpose of this study is to answer this question with regard to the use of compression seals in concrete pavements.

The evaluation of joint conditions after years of exposure required that we find projects or adjacent projects that were structurally the same. The joint sealant would be the only variable. We were fortunate in finding five locations where direct comparisons could be made. Each of these projects was more than 2 miles in length and contained neoprene compression seals. Each project contained numerous joints, which made it easy to reach conclusions concerning relative joint conditions. All of the seals were made by the same manufacturer.

Photographs were taken of joints at random to verify their general conditions. Thirty to 40 pictures were taken of each state's installation; the photographs shown in this report generally summarize the conditions that were found.

SEALING SYSTEM SURVEY

Minnesota

The first commercial neoprene compression sealed joints used in Minnesota highways were placed in the late fall of 1964 on I-90 in the westbound lanes starting at the west side of the Mississippi River Bridge and extending to Dresbach, Minnesota. The seals were installed manually. Both $^{11}/_{16}$- and $^{13}/_{16}$-in. materials were placed in $^{3}/_{8}$-in. joints at 46½-ft spacings. Figure 1 shows a typical joint in the eastbound lanes sealed with two-component polysulfide material; Figure 2 shows a typical joint sealed with neoprene. All of the polysulfide-sealed joints show spalls where the faces of the joint break away (Fig. 3) because, although adhesion of the joint material is excellent in places, the extensibility of polysulfide joints is limited. The neoprene-sealed joints show slight raveling of the joint edges, particularly where the seal is installed deeper than $^{1}/_{8}$ in. below the pavement surface (Fig. 4).

Figure 5 shows that polysulfide sealant material becomes embedded with incompressible stones and debris. Adhesion to the faces of the joint was nonexistent in most areas.

Figure 6 shows a neoprene seal after 7 years of service. The seal was of a tapered design and was replaced in later installations by a parallel-sided design that gave greater surface contact for holding the seal in the joint. Note that the joint below the seal is clean. The ruptured lubricant film has been forced to the bottom of the joint by the insertion of the seal in squeegee-like fashion.

Care must be exercised in the placing of neoprene to prevent stretching of the seal. Figure 7 shows a typical break that was caused by excessive stretching of the seal due to manual methods. These openings allow incompressible debris to enter the joint.

Sponsored by Committee on Sealants and Fillers for Joints and Cracks.

Figure 1. Polysulfide-sealed joint.

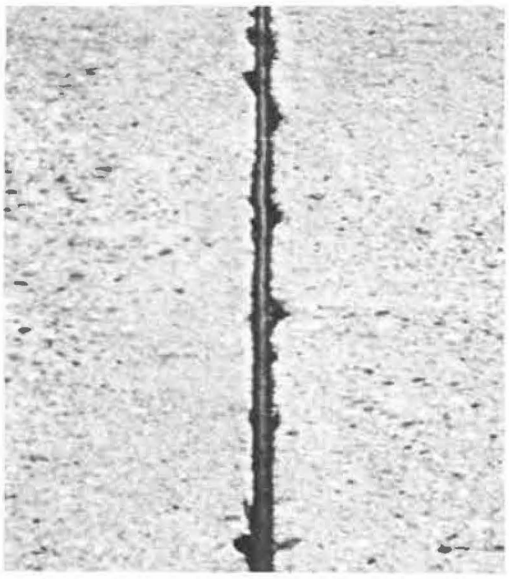

Figure 2. Neoprene-sealed joint.

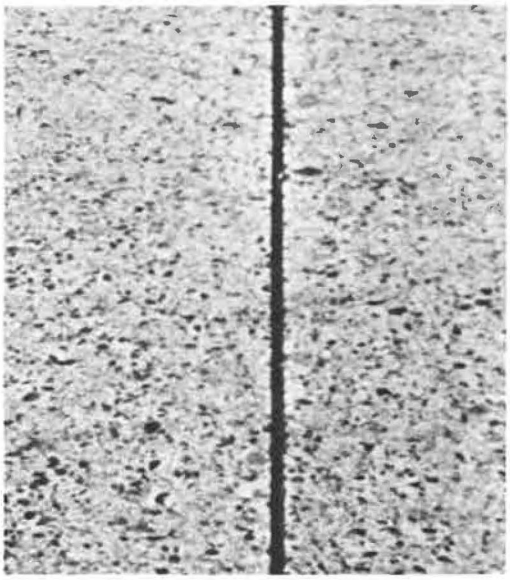

Figure 3. Polysulfide-sealed joint with spalls.

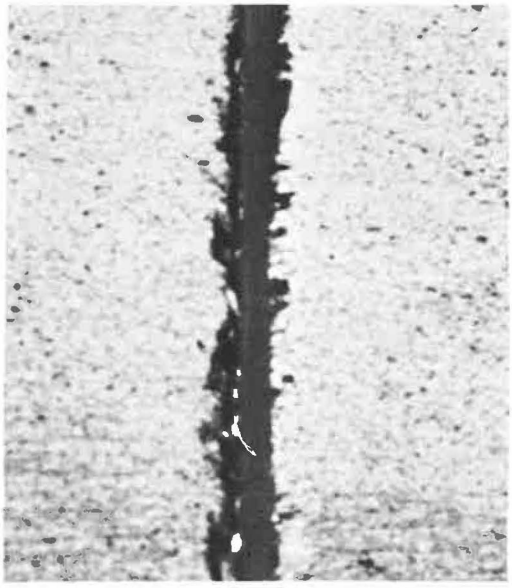

Figure 4. Neoprene-sealed joint with ravels.

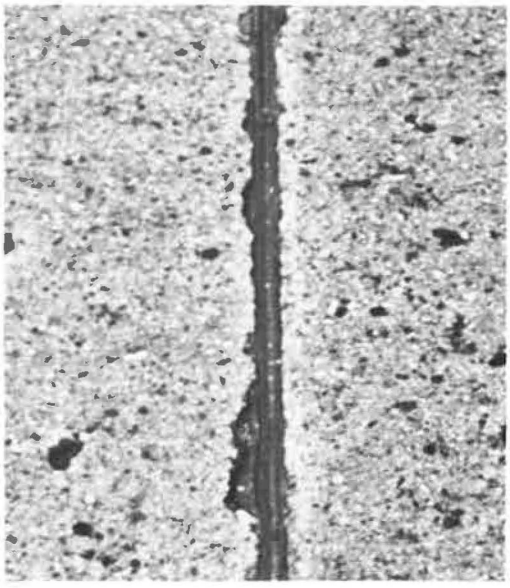

Figure 5. Polysulfide seal with embedded debris.

Figure 6. Neoprene seal.

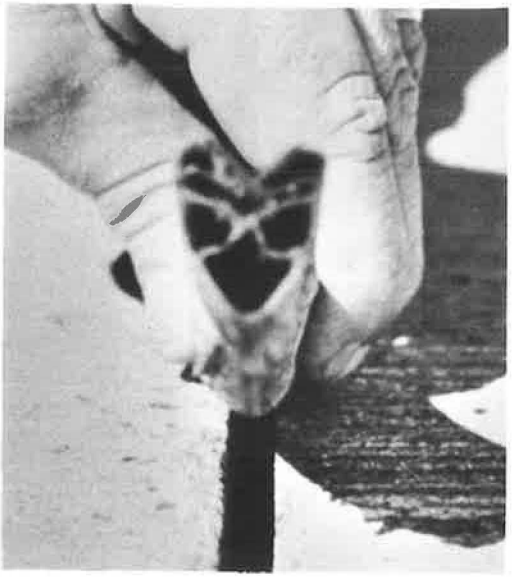

Figure 7. Break in neoprene seal.

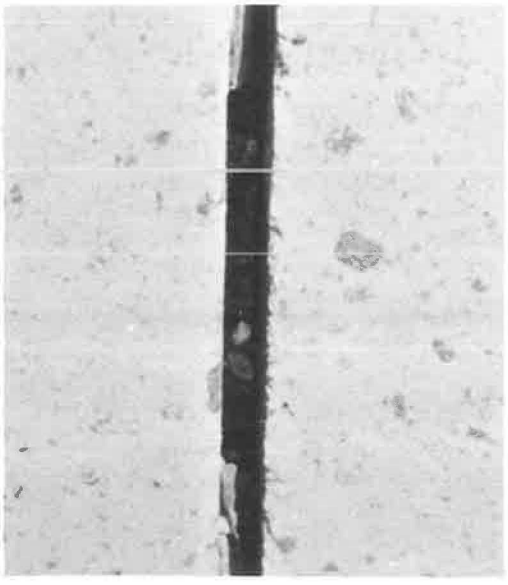

North Dakota

The first project to utilize neoprene compression seals in North Dakota was completed in 1964. The seals were installed by hand; $^{13}/_{16}$-in. materials was used at 45-ft spacings. The sections, more than 1 mile each, were placed in westbound I-94, west of Sweet Briar Dam. Three types of sealants were used in each: hot-poured asphalt, coal-tar epoxy, and neoprene compression seals. After 1 year, the neoprene was the only seal still working. Because of the extreme temperature range experienced, however, the seal size was increased to a width of $1\frac{1}{4}$ in. to facilitate large joint movement.

Figure 8 shows a hot-poured asphalt-sealed joint after 7 years of service. Figure 9 shows a neoprene-sealed joint of like service. Figure 10 shows a coal-tar epoxy joint that has spalls at intermittent points. Figure 11 shows a 1-in. wide liquid-sealed joint. A large sponge insert was used to gain a shape factor. Figure 12 shows a hot-poured joint that is full of incompressible material. This material contributes to the rapid deterioration of the joint faces.

Figure 13 shows a neoprene seal pulled after 7 years of service. The joint faces are clean and smooth, and the seal is fully resilient.

Figure 8. Hot-poured asphalt-sealed joint.

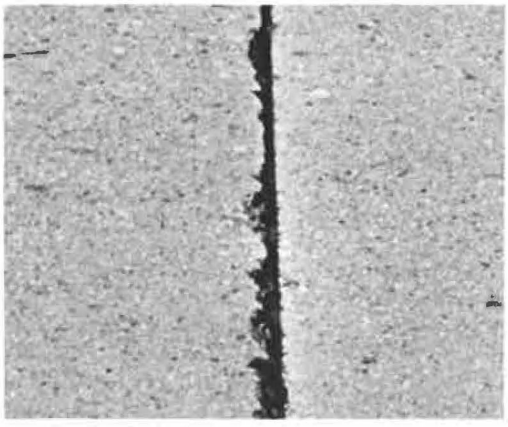

Figure 9. Neoprene-sealed joint.

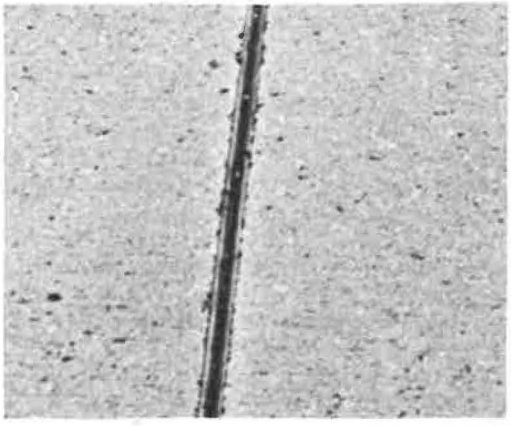

Figure 10. Coal-tar epoxy joint.

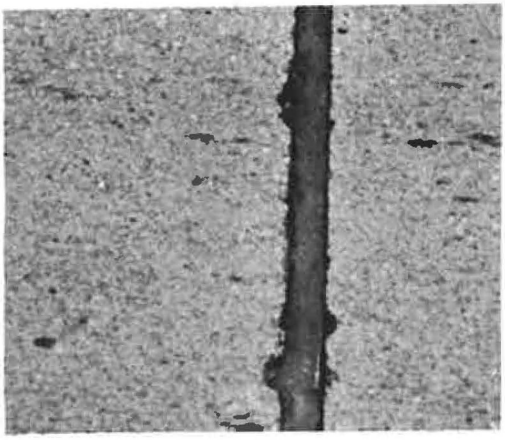

Figure 11. Liquid-sealed joint.

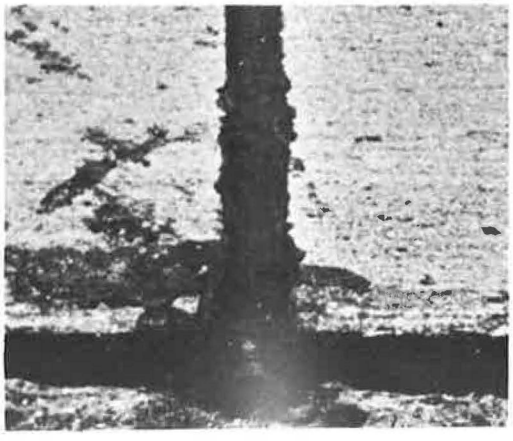

Figure 12. Hot-poured joint.

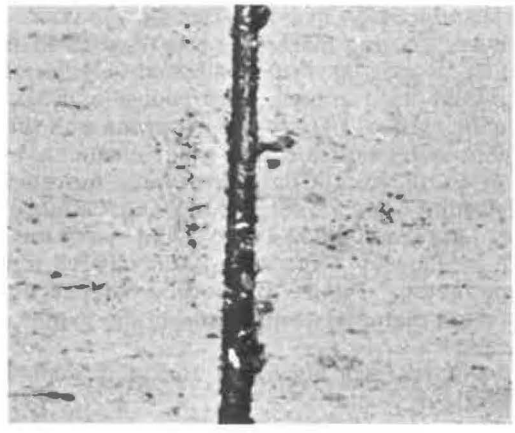

Figure 13. Neoprene seal.

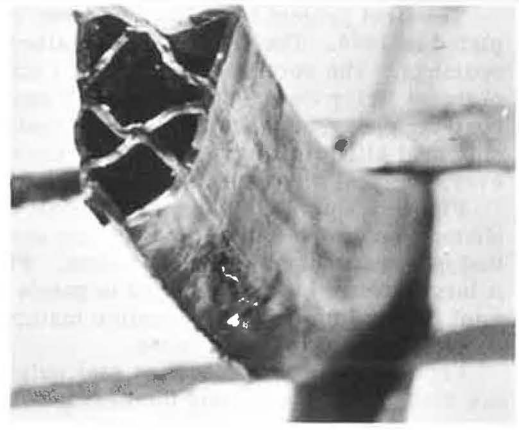

Michigan

Prior to adopting neoprene compression seals as the standard seal for all jointed pavement in 1965, Michigan specified hot-poured rubber asphalt as the standard material. Figure 14 shows a typical asphalt joint that has been resealed with SAO asphalt; Figure 15 shows a section of pavement sealed with neoprene. A seal 1¼ in. wide was used in ½-in. styrofoam-formed joints at 71-ft joint spacings. This was the first major neoprene project in the state. It was accomplished by machine in the fall of 1964. Machine placement provides uniform depth control and eliminates stretching. It is defined as the placing of a seal from a roll or strip automatically into the pavement slab without manual or outside assistance (force).

Figure 16 shows the ability of a neoprene compression seal of proper design and size to conform to small irregularities in the joint face. The pavement surface in this figure shows the effect of studded-tire wear. Figure 17 shows a joint with the compression seal removed. The joint is clean, and the plane-of-weakness crack is closed. There is no infiltration of debris.

Figure 18 shows a blowup that was repaired in the asphalt-sealed section immediately adjacent to the neoprene-sealed section. No blowups have occurred in the neoprene-sealed sections.

Figure 14. Resealed asphalt-sealed joint.

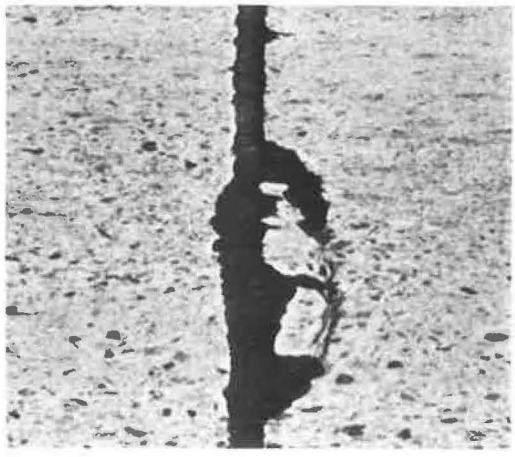

Figure 15. Neoprene-sealed joint.

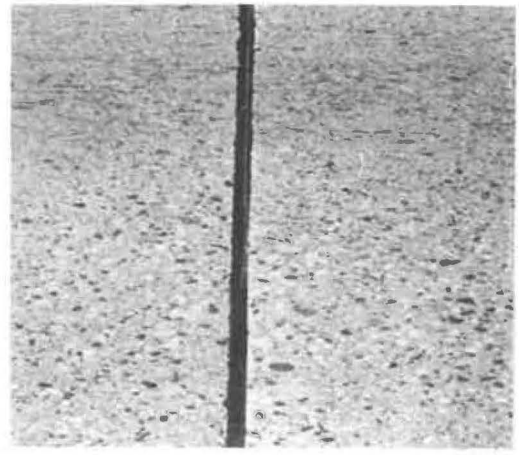

Figure 16. Neoprene conforming to irregular joint.

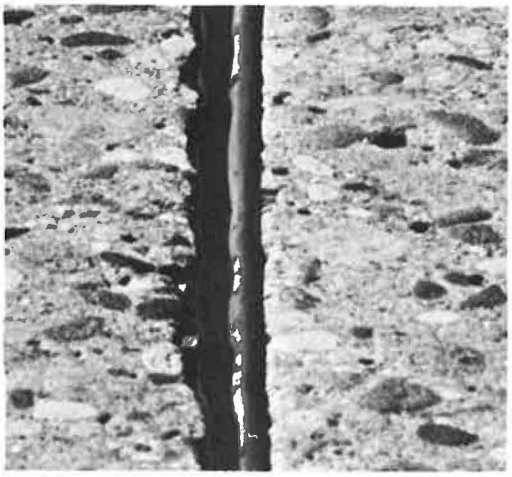

Figure 17. Clean joint with plane-of-weakness crack closed.

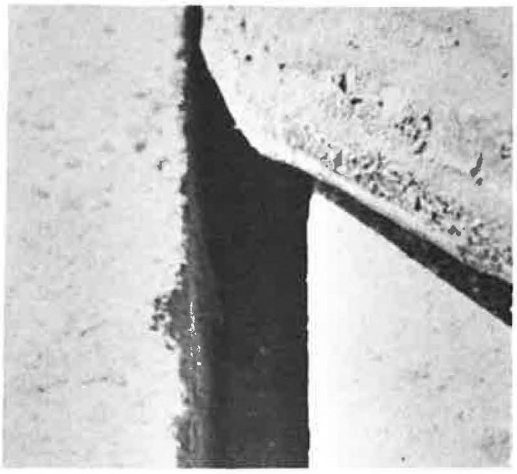

Figure 18. Blowup patch.

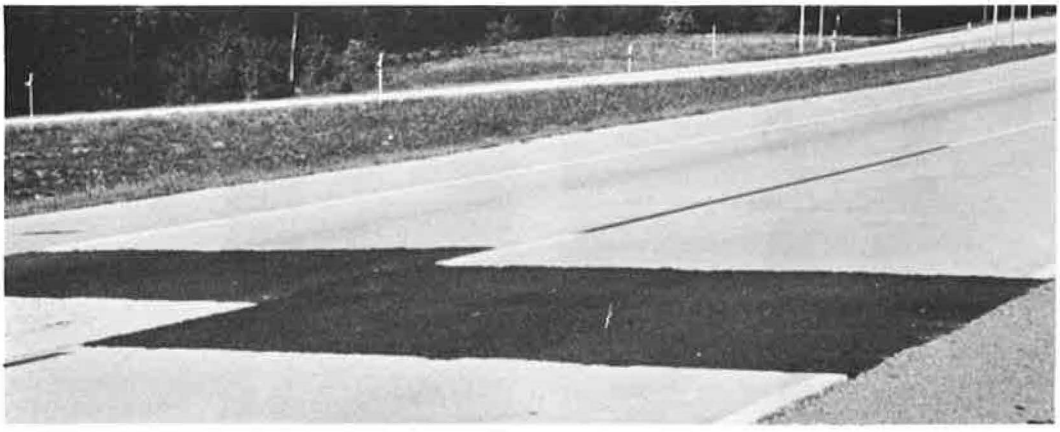

Ohio

Ohio's first project using neoprene compression seals was built in the spring and summer of 1965 on US-23 around Upper Sandusky. An $^{11}/_{16}$-in. compression seal was used in $^{1}/_{4}$-in. joints on 60-ft centers for the transverse contraction joints. The $^{1}/_{8}$-in. longitudinal joint was sealed with $^{5}/_{16}$-in. neoprene.

Figure 19 shows a liquid-sealed joint in the section of pavement adjacent to the neoprene-sealed section. Figure 20 shows a typical neoprene-sealed joint. The liquid-sealed section of pavement is approximately 1 year older than the neoprene section.

An inspection of the liquid-sealed joints shows a considerable amount of compacted debris in the joints, which causes substantial edge spalling of the joints (Fig. 21). Figure 22 shows that such an accumulation of debris in the neoprene-sealed joint is impossible because of lack of space. A longitudinal joint was sealed with neoprene; the joint shows no signs of spalling or deterioration (Fig. 23).

The longitudinal joint was sealed with neoprene on this project and shows no signs of spalling or deterioration, as shown in Figure 23.

Figure 19. Liquid-sealed joint with spalls.

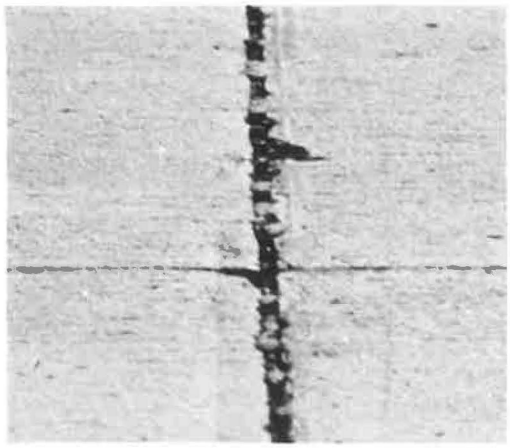

Figure 20. Neoprene-sealed joint.

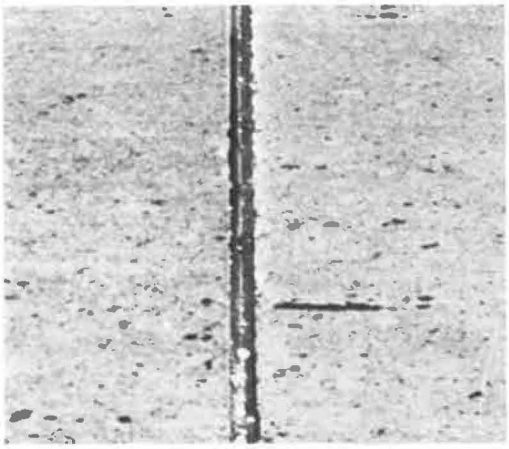

Figure 21. Incompressible materials causing spalls.

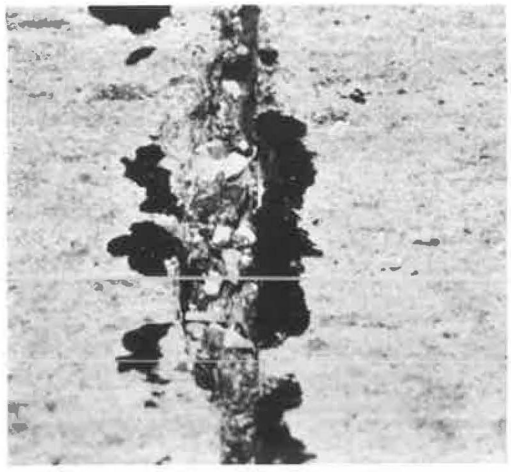

Figure 22. Neoprene-sealed joint at optimum depth.

Figure 23. Longitudinal joint sealed with neoprene.

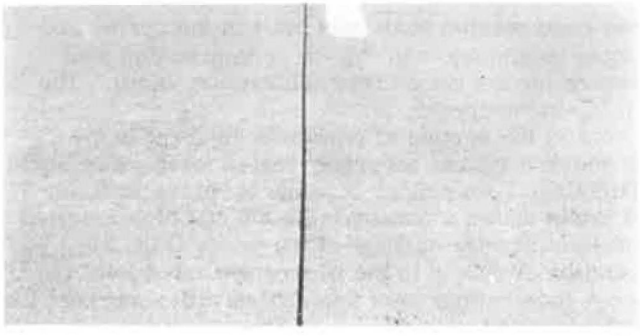

California

In 1964, a 4-mile section containing neoprene compression seals was placed in I-80 in the Donner Summit area. In addition, within this area 3 sections, containing 12 joints each, were sealed with a two-component polysulfide type of material that is used at elevations above 3,500 ft. Three sections, containing 12 joints each, were left unsealed as is standard below elevations of 3,500 ft (commonly referred to as valley areas).

All of the joints were sawed on a skew of 4 ft in 24 ft. They were sawed $\frac{1}{8}$ to $\frac{3}{32}$ in. wide and placed at an average of 15-ft spacings. In the case of the neoprene joints, seals $\frac{5}{16}$ in. wide were used. They were hand installed by the roller tool method.

Of all the joints surveyed in this study, these were the worst. At this installation, there is excessive pavement wear and subsequent joint abrasion because the use of chains is required for nearly 3 months following periods of snowfall.

Figure 24 shows an unsealed joint in a truck lane. Figures 25 and 26 show polysulfide-sealed and neoprene-sealed joints in a truck lane. The loss of material at the joint edges exposed the neoprene to traffic that abraded the seal to the extent that the upper portions were shredded off. The polysulfide was completely pulled from the joints in places.

Figure 27 shows an unsealed joint in a passing lane. Although the joint edges are not rounded and worn, considerable damage has occurred to the joint as a result of compaction of incompressible material into the joint. The width of the joint, originally $\frac{1}{8}$ in., is now at least $\frac{1}{4}$ in. Without exception, all unsealed joints were twice the width

Figure 24. Unsealed joint (truck lane).

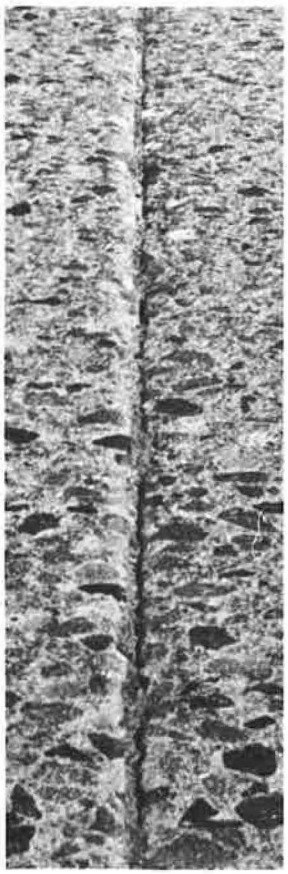

Figure 25. Polysulfide-sealed joint (truck lane).

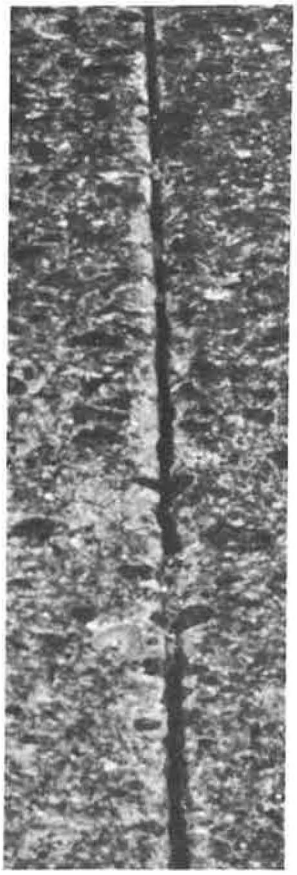

Figure 26. Neoprene-sealed joint (truck lane).

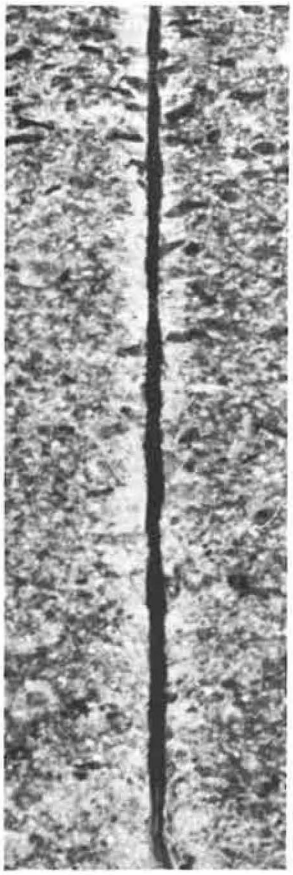

Figure 27. Unsealed joint (passing lane).

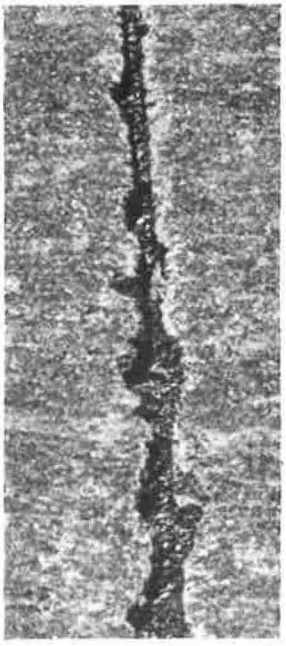

Figure 28. Polysulfide-sealed joint (passing lane).

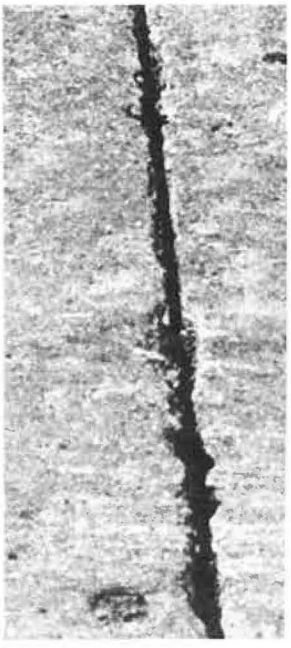

Figure 29. Neoprene-sealed joint (passing lane).

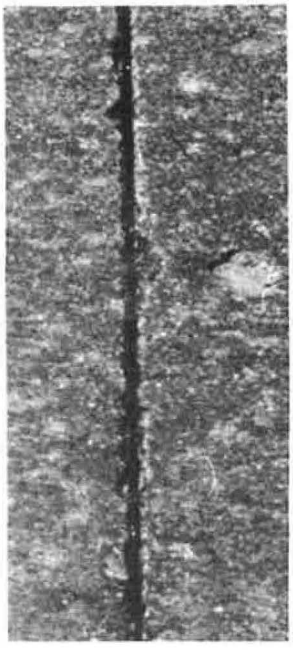

Figure 30. Close-up of unsealed joint (truck lane).

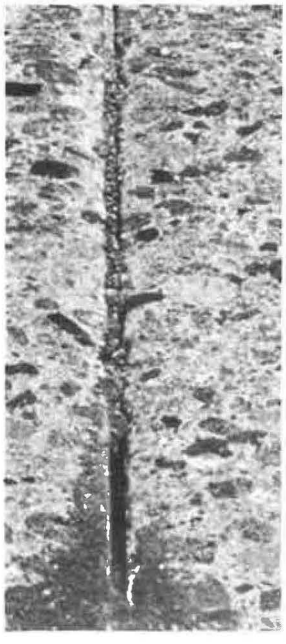

Figure 31. Close-up of polysulfide-sealed joint (truck lane).

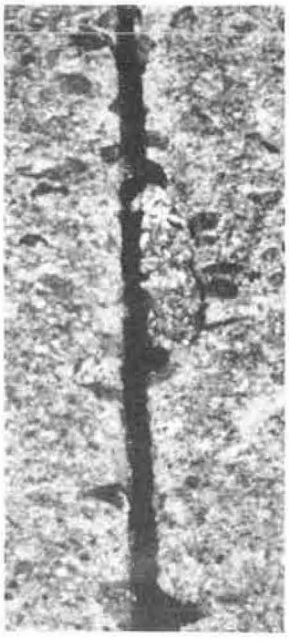

Figure 32. Close-up of neoprene-sealed joint (truck lane).

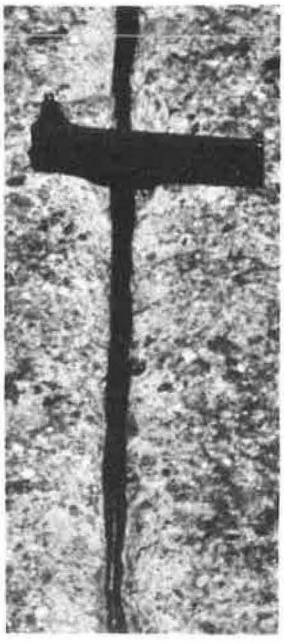

Figure 33. Unsealed joint prior to coring.

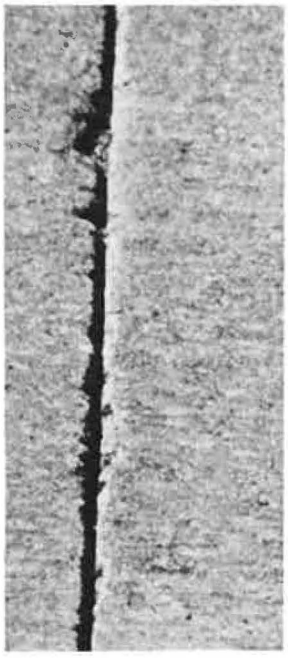

Figure 34. Close-up of core area (unsealed joint).

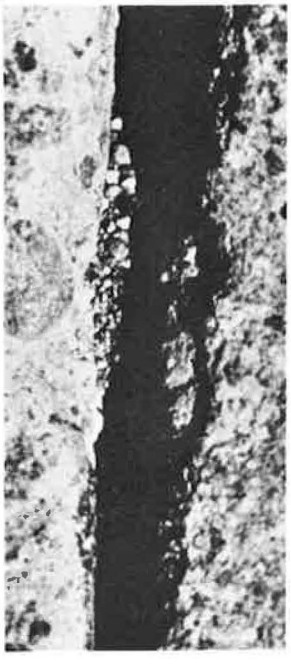

Figure 35. Damaged plane-of-weakness crack (unsealed joint).

Figure 36. Polysulfide-sealed joint prior to coring.

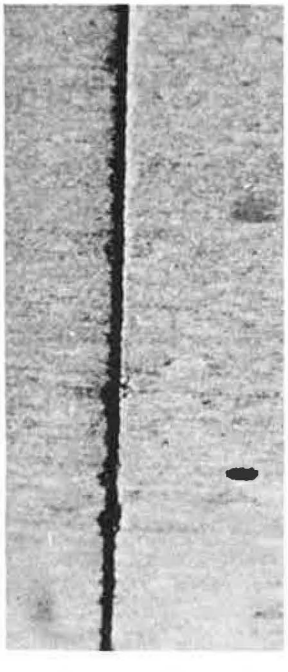

Figure 37. Close-up of core area (polysulfide-sealed joint).

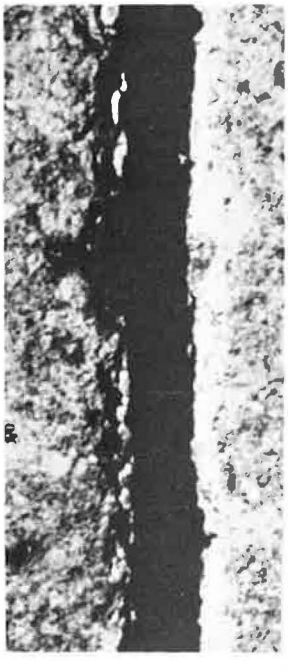

Figure 38. Plane-of-weakness crack (polysulfide-sealed joint).

Figure 39. Neoprene-sealed joint with raveled edges.

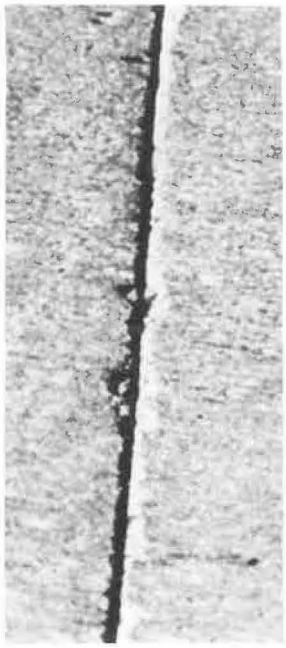

Figure 40. Close-up of core area (neoprene-sealed joint).

Figure 41. Undamaged core (neoprene-sealed joint).

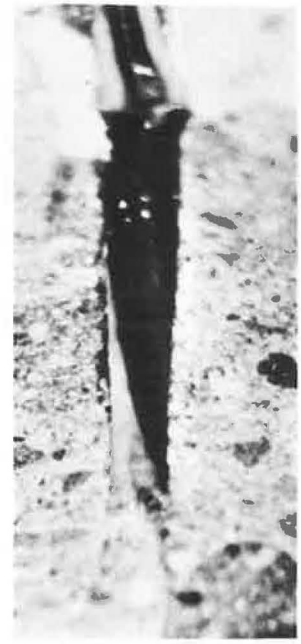

of the neoprene-sealed joints. A comparison of polysulfide-sealed and neoprene-sealed joints in passing lanes is shown in Figures 28 and 29.

Figures 30, 31, and 32 show three types of joints in truck lanes: open or unsealed, polysulfide, and neoprene. The 3-in. rule across the neoprene-sealed joint indicates the extent of edge wear.

The California Division of Highways conducted core tests of the different types of joints. The following pictures are the results of the test program.

Figure 33 shows an unsealed joint prior to coring; Figure 34 shows the core area. Incompressible material can be seen in the joint; however, much of this material was washed away during the coring operation. Figure 35 shows the core hole and the damage caused by the compaction of incompressible material at the bottom of the sawed joint following the plane-of-weakness crack. This accounts for the excessive width of the unsealed joints.

Figure 36 shows a polysulfide-sealed joint prior to coring. Figure 37 shows the core area, and Figure 38 shows the hole with the core removed. Again, there is considerable infiltration, and the plane-of-weakness crack has been forced open.

Figure 39 shows a neoprene-sealed joint that is raveled along the joint edges. Although the upper edges of the seal are shredded (Fig. 40), the seal is still effective because incompressible material has been kept out of the plane-of-weakness crack (Fig. 41). The fact that the neoprene-sealed joints were tight and that the plane-of-weakness crack was able to close completely raises the question of whether much infiltration occurs from the bottom of the joint, especially with cement-treated subbases such as were used here.

Although only one joint of each type is shown here, cores were taken from several joints of each type, and the results were comparable in each case.

CONCLUSIONS

Neoprene seals, by keeping incompressible materials and liquids that carry fine debris and silt from the plane-of-weakness cracks, can prevent functional damage to

joints and thereby extend the life of a structure. This statement cannot be made for the other systems observed in this study. In the five states surveyed in this report, the joints sealed with neoprene were in better overall condition than those sealed with other systems. Minnesota research engineers stated that 98 to 99 percent of their problems with joints have been eliminated since they started using neoprene seals.

No blowups have occurred in the neoprene-sealed sections of pavement under study; however, blowups have occurred in the adjacent sections.

The joints in California that contained no sealant of any type are now at least twice their original width.

Unsealed and liquid-sealed joints showed considerable degradation and damage through the infiltration of incompressible material into the joints. After 6 or 7 years of service, repair or rehabilitation of the joints would be impossible because of the infiltration of incompressible material into the plane-of-weakness cracks. Further damage might be stopped by adequate sealing. A survey should be made in 2 to 3 years to determine the extent of the damage to the slabs. Slab damage is currently minimal with all systems.

ACKNOWLEDGMENTS

I would like to thank the following men for their assistance: D. L. Spellman and L. S. Spickelmire, California Division of Highways; L. T. Oehler and F. J. Bashore, Michigan Department of State Highways; P. J. Diethelm and P. C. Hughes, Minnesota Department of Highways; C. E. Rice and D. L. Schwichtenberg, North Dakota State Highway Department; and W. J. Anderson and J. T. Paxton, Ohio Department of Highways.

VISCOELASTIC MODEL FOR ELASTOMERIC PAVEMENT JOINT SEALS

Ravindra K. Vyas, University of Utah

This paper describes the development of a simple viscoelastic model to simulate the time-dependent behavior of elastomeric seals. The model chosen for demonstration is the 3-parameter solid. Standard responses of this model are briefly described and are followed by appropriate analytical expressions. The analytical expressions are given in a general form and refer to three particular cases: (a) response to a fixed level of deformation that has been held for a specified length of time, (b) response on release from such a fixed level of deformation, and (c) load-deflection response in an experiment at a constant rate of displacement. The required parameters of the model are evaluated by using the experimental values obtained for an actual seal. The performance of the seal is then compared with that of the model. The model enables us to make some important acceptable predictions: (a) residual deformations immediately on release from a fixed level of compression, (b) the subsequent recovery of the seal as a function of time, (c) the decay of the effective force exerted by the seal, and (d) the effect of the displacement rate on the load-deflection characteristic. Suggestions for further refinement of the model are also given.

•AN efficient pavement joint seal should at all times be in contact with the sides of the joint opening and should maintain adequate pressure on the seal-pavement interface to prevent the intrusion of water and incompressible materials into the joint opening (6, 7, 8). To function effectively, the seal must be able to expand quickly to bridge any opening created by slab movement. At the same time, it must also maintain effective contact with the sidewalls and exert adequate pressure to meet the requirement previously described.

A variety of solid and liquid pavement sealers are commercially available and have been discussed in adequate detail elsewhere (1, 2, 5, 6, 8). In a recent study, conducted by the author (7, 8), it was observed that elastomeric seals combine flexibility with resilience and seem to be well suited for effectively sealing pavement joints.

The principal items of interest to the highway engineer are the maximum tensile and compressive stresses in a given seal and the effective pressure exerted by the seal on the sidewalls of the joint opening. The maximum stresses in a seal can be evaluated analytically (7, 8) or experimentally by using the photoelastic method (3). The effective pressure exerted by the seal is usually assessed by short-time load-deflection experiments conducted in the laboratory. Although these experiments give a fair idea of the strength of the seal, it is important to recognize that the basic seal material is viscoelastic (1, 2, 7, 8). Consequently, the effective pressure exerted by the seal on the interface will vary with time. Little is known about the correct constitutive relationships that relate the stresses and strains in the basic seal material. It is possible, however, to develop tentative working models that give a better understanding of the product and its performance.

Sponsored by Committee on Sealants and Fillers for Joints and Cracks.

The results of the experimental studies on the recovery of preformed elastomeric seals emphasize two salient features of the seals. When released from a fixed level of deformation that has been held for a specified duration of time, the seals show a definite (but not complete) recovery immediately on release. As a result, all seals tested show a residual deformation that is temporary in nature and that, in most cases, is fully recovered with lapse of time. These findings indicate that the behavior of the product is comparable to that of a viscoelastic solid (8). The simplest possible viscoelastic model that can simulate this behavior is the 3-parameter solid (4) shown in Figure 1.

The main objective of this paper is to simulate the behavior of a seal by means of the viscoelastic model previously mentioned. The necessary mathematical expressions for the 3-parameter solid are developed for three different situations: (a) response to a fixed level of deformation that has been held for a specified duration of time, (b) response on release from such a given level of deformation, and (c) response of the model in a load-deflection experiment conducted at a fixed displacement rate. The mathematical results are presented in a general form suitable for repeated use. The actual response of the model (Fig. 1) will depend on the values of the parameters k_1, k_2, and c associated with the springs and the dashpots shown in the figure. In a more general form, these parameters are designated by the symobols β_1, β_2, and γ. For practical predictions, the parameters are evaluated from the experimental results obtained for an actual seal. The performance of the corresponding model, so constructed, is then compared with the actual response of the sample. The model is used, subsequently, to predict the effective force exerted by the seal with lapse of time when it is held at a fixed level of deformation. Further, the same model is used to construct the load-deflection curves for a similar seal when tested at different displacement rates.

DESCRIPTION OF THE MODEL

The model for the 3-parameter solid (Fig. 1) is composed of a linear spring k_1 in series with a Kelvin solid (4). The latter consists of a linear spring k_2 in parallel with a dashpot whose constitutive constant is c. The symbol c is meant to indicate that the resistance offered by the dashpot is equal to the product of this constant and the time rate of displacement in the dashpot. We may, for the sake of convenience, refer to a dashpot with a high value of c as a stiff dashpot and a dashpot with a low value of c as a weak dashpot. Further, we designate by ℓ the distance between terminals A and B, when the model is completely free of stress. When such a stress-free model is subjected to a load P(t), the spring k_1 and the Kelvin element undergo displacements $\delta_1(t)$ and $\delta_2(t)$, as shown in Figure 1. These displacements are governed by the following relationships:

$$k_1\delta_1(t) = P(t) \tag{1}$$

$$k_2\delta_2(t) + c\dot{\delta}_2(t) = P(t) \tag{2}$$

where

$$\dot{(\ )} = d/dt(\ ) \tag{3}$$

Equation 3 defines the dot notation for designating the time derivative of a function. The total displacement $\delta(t)$ in the model is given by

$$\delta(t) = \delta_1(t) + \delta_2(t) \tag{4}$$

As implied in Eqs. 1 through 4, forces and displacements are treated as functions of time t. We introduce, next, dimensionless displacements as follows:

$$x_1(t) = \delta_1(t)/\ell \tag{5}$$

Figure 1. The 3-parameter solid.

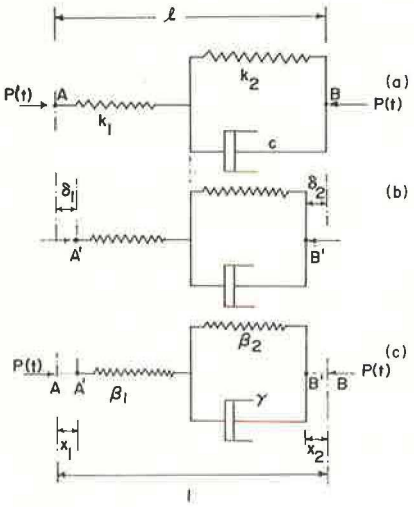

Figure 2. Deformation under a step load of one unit.

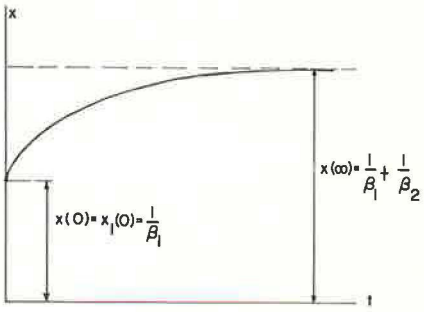

Figure 3. Effective load P(t) when model is subjected to a fixed deformation x_o.

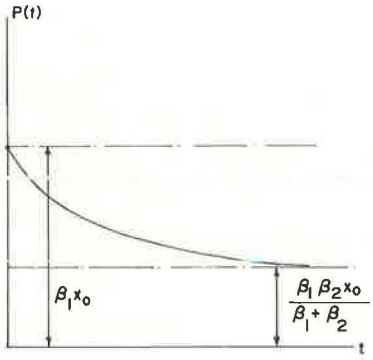

Figure 4. Response of model on release from deformation x_o, held for a duration of time τ.

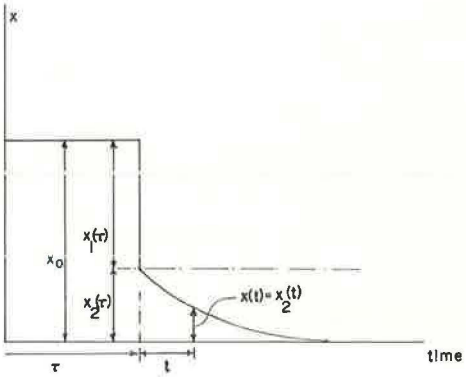

Table 1. Recovery results for a sample at 0 F and 40 percent nominal deformation.

	Observed Values of $x(t) = x_2(t)$ on Release From Deformation x		
Time t (min)	τ^a = 24 hours x^b = 0.424	τ = 48 hours x = 0.398[c]	τ = 168 hours x = 0.398[c]
0	0.154	0.156[c]	0.193
1	0.124	0.097	0.150
2	0.092	0.087	0.139
3	0.088	0.077	0.130
4	0.082	0.069	0.115
5	0.082	0.066	0.110
10	0.076	0.053	0.099

[a]Duration τ in hours.
[b]Fixed deformation x in the duration τ.
[c]Values were used in evaluating the required parameters of the viscoelastic model.

$$x_2(t) = \delta_2(t)/\ell \tag{6}$$

$$x(t) = \delta(t)/\ell \tag{7}$$

Further, let

$$\beta_1 = \ell k_1 \tag{8}$$

$$\beta_2 = \ell k_2 \tag{9}$$

$$\gamma = \ell c \tag{10}$$

By using Eqs. 5 through 10, Eqs. 1, 2, and 4 may be rewritten as

$$\beta_1 x_1(t) = P(t) \tag{11}$$

$$\beta_2 x_2(t) + \gamma \dot{x}_2(t) = P(t) \tag{12}$$

$$x(t) = x_1(t) + x_2(t) \tag{13}$$

In Eqs. 11 through 13, x is related to the total percentage of compression in the model; x_1 and x_2 are related to the contribution from the two components of the basic model. We may look on these expressions as providing a description of the performance of the normalized model shown in Figure 1c.

The 3-parameter solid is a basic viscoelastic model and is very adequately described elsewhere (4). Some salient features of the model are as follows. When the model is subjected to a unit step load, the linear spring β_1 responds immediately with an initial displacement $x = 1/\beta_1$, which is followed by viscous creep (Fig. 2). If, on the other hand, the model is subjected to a fixed displacement x_0, the force required to maintain this displacement diminishes exponentially as shown in Figure 3. The response of the model on release from such a fixed displacement x_0, held for a duration of time τ, is shown in Figure 4. As this figure shows, the elastic component $x_1(\tau)$ is recovered immediately, whereas the Kelvin component $x_2(\tau)$ is recovered exponentially with lapse of time from release. The eventual recovery of this Kelvin component is an important feature of the response and is responsible for the designation of the model as a viscoelastic solid.

ANALYTICAL EXPRESSIONS FOR THE THREE CASES

The behavior described in the preceding section compares favorably with that observed experimentally for elastomeric seals. The expressions given in this section will be helpful in finding a working 3-parameter model for a given seal. All of the expressions are derived from Eqs. 11 through 13 by using appropriate conditions for each particular case.

Case One

Displacement x_0 held for time τ.

Conditions:

$$x(0) = x_1(0) = x_0 \tag{14}$$

$$x_2(0) = 0 \tag{15}$$

$$t \leq \tau \tag{16}$$

Solutions:

$$x_2(t) = [\beta_1/(\beta_1 + \beta_2)]\ x_0\ [1 - e^{-at}] \tag{17}$$

$$x_1(t) = [\ \beta_1/(\beta_1 + \beta_2)]\ x_0\ [(\beta_2/\beta_1) + e^{-at}] \tag{18}$$

$$P(t) = [\ \beta_1/(\beta_1 + \beta_2)]\ x_0\ [\beta_2 + \beta_1 e^{-at}] \tag{19}$$

where

$$a = (\beta_1 + \beta_2)/\gamma \tag{20}$$

Case Two

Response on release from a displacement x_0 held for time τ. In case two we have to proceed from the information obtained from case one. From the basic character of the model, we recognize that as soon as the displacement x_0 is released, after it has been held for duration τ, there will be an immediate recovery equal in magnitude to $x_1(\tau)$. The displacement $x_2(\tau)$ will appear as a residual deformation, which will be recovered eventually with lapse of time. Then, for this case, we have the following situation.

Conditions:

$$t > 0_+ \text{ (measured from the instant of release)} \tag{21}$$

$$P(t) = 0 \tag{22}$$

$$x_2(0) = x_2(\tau) \tag{23}$$

where $x_2(\tau)$ is obtained from Eq. 17.

Solutions:

$$x(t) = x_2(t) = x_2(\tau)e^{-(\beta_2/\gamma)\ t} \tag{24}$$

Case Three

Load-deflection response in a test at constant rate of displacement α.

Conditions:

$$\alpha = \text{imposed displacement rate (units of length/units of time)} \tag{25}$$

$$\dot{x} = \alpha/\ell \tag{26}$$

$$x(0) = x_1(0) = x_2(0) = \dot{x}_2(0) = 0 \tag{27}$$

Solutions:

$$x_1(x) = (\beta_1\alpha/\gamma a^2\ell)\left[1 + (\beta_2/\beta_1)\ (a\ell/\alpha)\ x - e^{-(a\ell/\alpha)x}\right] \tag{28}$$

$$x_2(x) = (\beta_1\alpha/\gamma a^2\ell)\left[e^{-(a\ell/\alpha)\ x} + (a\ell/\alpha)\ x - 1\right] \tag{29}$$

$$P(x) = (\beta_1^2 \alpha / a^2 \gamma \ell) \left[1 + (\beta_2/\beta_1)(a\ell/\alpha) x - e^{-(a\ell/\alpha) x} \right] \quad (30)$$

or

$$u(x) = \alpha \left[1 + (\beta_2/\beta_1)(a\ell/\alpha) x - e^{-(a\ell/\alpha) x} \right] \quad (31)$$

where

$$u(x) = \left[P(x) a^2 \gamma \ell \right] / \beta_1^2 \quad (32)$$

APPLICATION TO ELASTOMERIC SEALS

The expressions derived in the preceding section are useful in predicting the time-dependent response of a unit length of an actual seal. For the purpose of such a prediction, however, we need the appropriate numerical values of the constants β_1, β_2, and γ or the ratios β_2/β_1, $\beta_1/(\beta_1 + \beta_2)$, $(\beta_1 + \beta_2)/\gamma$, and β_2/γ. These ratios can be easily evaluated from the results of recovery experiments for an actual seal.

In a recent study conducted by the author (8), a number of seals were tested at 0, 75, and 120 F for their recovery as a function of time on release from fixed levels of deformation that had been held for specified durations of time. The recovery of all the seals tested was found to be weakest at the low temperature of 0 F. Some results for one of the seals, tested at 0 F, are given in Table 1. These results are used in the numerical example that follows to evaluate the ratios mentioned previously. It should be noted that the corresponding model applies to a rather stringent practical situation.

When the sample is held at 39.8 percent deformation (Table 1) for 48 hours, or 2,880 minutes, and then released, it has a temporary residual deformation of 15.6 percent. By using this information in Eq. 17, we get

$$\left[\beta_1/(\beta_1 + \beta_2) \right] \left[1 - e^{-2880\,a} \right] = 0.156/0.398 = 0.392 \quad (33)$$

Similarly, from the results of the 168-hour (1-week) test

$$\left[\beta_1/(\beta_1 + \beta_2) \right] \left[1 - e^{-10080\,a} \right] = 0.193/0.398 = 0.485 \quad (34)$$

In Eqs. 33 and 34, we have two equations and two unknown quantities, $\beta_1/(\beta_1 + \beta_2)$ and a. These equations can be solved quickly by the following iterative scheme. We first solve Eq. 34 for $\beta_1/(\beta_1 + \beta_2)$, assuming that the contribution from the exponential term is negliglible. Then, we use this value in Eq. 33 to evaluate a. Next, we substitute the value of a in Eq. 34 to reevaluate $\beta_1/(\beta_1 + \beta_2)$ for the second iteration. This iterative process is continued until satisfactory convergent values are obtained for the two unknowns. In the present example, we converge to the following values at the end of two cycles

$$\left[(\beta_1 + \beta_2)/\beta_1 \right] = 2.06, \quad \beta_2/\beta_1 = 1.06, \quad a = 0.571 \times 10^{-3} \quad (35)$$

Next, we consider the response of the seal on release from 39.8 percent compression (held for 48 hours). From the value at t = 0 (Table 1, column 3) and Eq. 24, we get

$$x_2(t) = x(t) = 0.156\, e^{-(\beta_2/\gamma)t} \quad (36)$$

where t = time in minutes from release. From these results (Table 1, column 3), we obtain the following average value for β_2/γ:

$$\beta_2/\gamma = 0.202 \quad (37)$$

It may be pointed out here that the model parameters are assumed to be temperature-dependent. The numerical values obtained in this example refer to a model that may be used to represent the particular seal considered at a temperature of 0 F.

DISCUSSION OF RESULTS

It is important to verify whether the model we have constructed is satisfactory. For this purpose we compare the response of the model with that observed for the seal. The comparison is shown in Figure 5 and Table 2. The plots in Figure 5 were constructed by using the model parameters already evaluated in Eqs. 35 and 37 and the observed values given in Table 1. From the plots, it is evident that the 3-parameter solid satisfactorily predicts the performance of the actual seal. The model predicts a more favorable recovery than that observed, but the differences are not large.

An important value from a practical standpoint is the residual deformation that occurs immediately on release. A comparison of these values for the model and the actual seal is given in Table 2. The last row in this table gives the largest deviation between the observed and the predicted values. The observed residual deformation in this case is 36.8 percent, whereas that predicted by the model is 29.3 percent, a difference of 7.5 percent. All the other values in this table show a deviation of less than ±4 percent. In view of the large deformations involved, the prediction made by the model is quite satisfactory.

As mentioned in the introduction, if the seal is to function effectively, it must maintain adequate force on the sidewalls of the joint. In this context, the results of the short-time load-deflection experiment and the use of the viscoelastic model yield some important information. From the load-deflection curve obtained by laboratory testing, the force P(0) exerted by the seal at a given percent deformation x can be readily obtained. When the seal is compressed to this same level of deformation in the pavement joint, it may be assumed that it exerts the same force P(0) on the interface at the time of installment. If the compression is maintained at all times, the seal, according to the model, will relax. Correspondingly, it will show a loss in the effective force exerted at the interface. From Eq. 19, the effective force P(t), after a lapse of time t from installment, is obtained as:

$$P(t) = P(0)\left[(\beta_2/\beta_1) + e^{-at}\right]/\left[(\beta_2/\beta_1) + 1\right] \qquad (38)$$

The foregoing relationship is shown in Figure 6. The effective force decays exponentially and reaches 51.5 percent of its initial value. This limiting value of the effective force is obtained by using β_2/β_1 (from Eq. 35) in Eq. 38 and proceeding to the limit as $t \to \infty$. It is interesting to note that the expression in Eq. 38 is independent of the imposed step displacement. We also notice that, for this seal, at the end of 3 days the effective force reduces to 52 percent of its initial value, which is very close to the limiting value. The result, in this particular case, supports the ASTM recommendation of a 72-hour recovery test at low temperature. However, the ASTM recommendation may be confirmed or revised only after the model parameters are carefully evaluated for a large variety of seals.

An important test used in assessing the strength of a given seal is the short-time load-deflection experiment. Most testing machines that are used in experimental work load the specimen at a constant rate of displacement. As indicated by Eq. 31, the displacement rate at which the specimen is tested does affect the load-deflection response. The seal for which we have evaluated the model parameters seems to have a very stiff dashpot. For such a model, the load-deflection response is not appreciably affected by a practical rate of loading. However, this characteristic curve will be significantly influenced by the rate of loading if we use a very weak dashpot in the model (Fig. 7). The curves in this figure are plotted for a model with a = 0.0571 (very weak dashpot). Other model parameters are assumed to be the same as those evaluated in the preceding section. When the model is tested at a displacement rate of α = 0.5 in./min, the viscous effects are almost imperceptible. However, as shown in Figure 7, the load values de-

Figure 5. Predicted and observed recovery of a seal at 0 F on release from 40 percent nominal deformation.

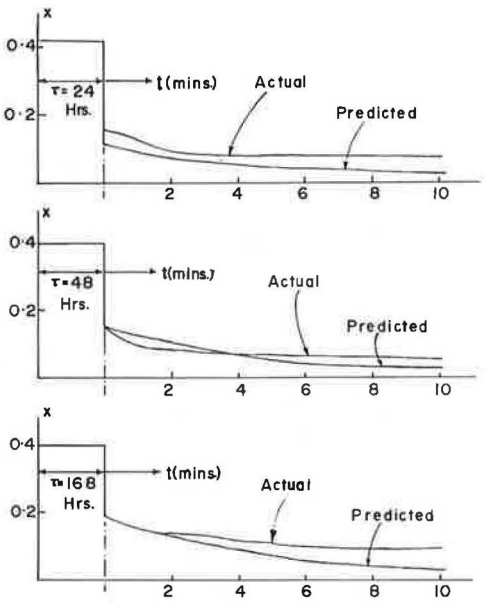

Table 2. Comparison of the actual immediate recovery of a seal and the recovery predicted by the model.

Test Duration τ (hour)	Nominal Deformation x Before Release (percent)	Values of x Immediately on Release	
		Actual Seal	Model Prediction
24	20	0.079	0.061
	40	0.154	0.116
	60	0.206	0.167
48	20	0.101	0.073
	40	0.156	0.156
	60	0.210	0.232
168	20	0.102	0.096
	40	0.193	0.193
	60	0.368	0.293

Figure 6. Predicted effective force P(t) at 0 F when the seal is held at a constant deformation.

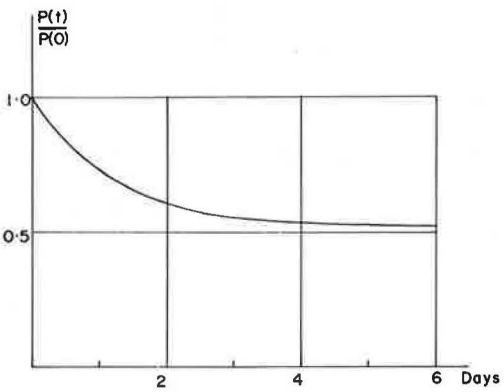

Figure 7. Load-deflection response in tests at different displacement rates.

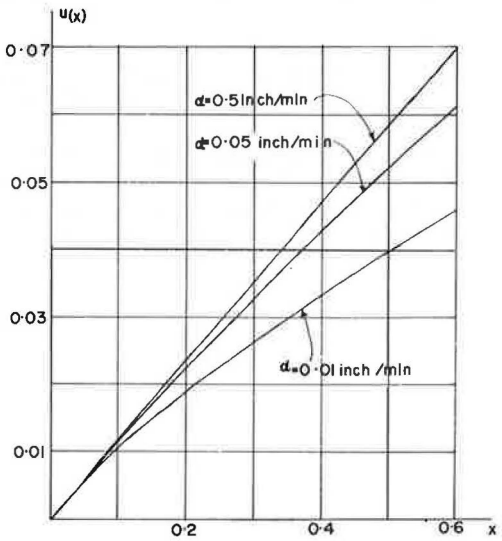

crease with a decrease in the loading rate. For example, for α = 0.05 in./min, the load at 40 percent compression will be 91 percent of its value when tested at α = 0.5 in./min. If the loading rate is reduced to 0.01 in./min, the corresponding load value will be reduced to 71 percent.

CONCLUDING REMARKS

Viscoelastic models can be effectively used to represent elastomeric seals. The 3-parameter solid described in this paper gives a good prediction of the time-dependent response of the product considered. It is worthwhile to note that we have used one of the simplest possible models to simulate the actual behavior of a given seal. Further refinements can be incorporated in the analysis by adding more Kelvin elements to the 3-parameter solid. With such complicated models it may be possible to simulate the time-dependent behavior of elastomeric seals much more accurately. A considerable additional amount of well-planned experimental work is necessary for the development of these more sophisticated models.

It has been pointed out elsewhere (7) that the short-time response of the seals can be predicted by a nonlinear analysis of the seal section as a structure. A corresponding modification can be incorporated in the viscoelastic model by using nonlinear springs. The analysis of the resulting model may become much more complicated; however, such a model may lead eventually to an optimum design of the product.

REFERENCES

1. Cook, J. P. A Study of Polysulfide Sealants for Joints in Bridges. Highway Research Record 80, 1965, pp. 11-35.
2. Cook, J. P., and Lewis, R. M. Evaluation of Pavement Joint and Crack Sealing Materials and Practices. NCHRP Rept. 38, 1967, 40 pp.
3. Cook, J. P. The Photoelastic Stress Analysis of a Preformed Compression Seal. Highway Research Record 320, 1970, pp. 1-8.
4. Flügge, W. Viscoelasticity. Blaisdell Publishing Co., 1967.
5. Hiss, J. G. F., Jr., Lambert, J. R., and McCarty, W. M. Joint Seal Materials: Final Report. Bureau of Physical Research, New York State Department of Transportation, Albany, Research Rept. 68-6, Dec. 1968.
6. Tons, E. A Theoretical Approach to Design of a Road Joint Seal. HRB Bull. 229, 1959, pp. 20-53.
7. Vyas, R. K. Analysis of Elastomeric Pavement Seals. Highway Research Record 357, 1971, pp. 72-79.
8. Vyas, R. K. Preformed Elastomeric Seals: Kinematics of Deformation and Some Basic Seal Properties. University of Utah Tech. Rept. UTEC CE 70-213, June 1971.

SPONSORSHIP OF THIS RECORD

GROUP 2—DESIGN AND CONSTRUCTION OF TRANSPORTATION FACILITIES
John L. Beaton, California Division of Highways, chairman

CONSTRUCTION SECTION
Robert D. Schmidt, Illinois Department of Transportation, chairman

Committee on Rigid Pavement Construction
John C. Dixon, Ohio Department of Highways, chairman
Harold E. Buckler, Don Cahoone, John H. Davis, Leet E. Denton, W. Stanley Ekern, Phil Fordyce, Gene K. Hallock, Harold Halm, S. E. Hicks, Emmett H. Karrer, Sanford P. LaHue, Bernard A. Lefeve, Robert J. Lowe, T. E. McElherne, William F. Mengel, Alving H. Meyer, August F. Muller, William G. Prince, Jr., Gordon K. Ray, Robert D. Schmidt, Peter Smith, James E. Wilson, Jr., William A. Yrjanson

GENERAL MATERIALS SECTION
F. E. Legg, Jr., University of Michigan, chairman

Committee on Sealants and Fillers for Joints and Cracks
John P. Cook, University of Cincinnati, chairman
J. N. Clary, Donald Dreher, Frank W. Eschmann, William T. Helm, Harry W. Johnson, John C. Killian, W. H. Larson, R. V. LeClerc, Leonard T. Norling, Edward R. Oglio, Dale E. Peterson, C. K. Preus, William G. Prince, Jr., Bernard A. Ross, John J. Schmitt, Raymond J. Schutz, Chris Seibel, Jr., Egons Tons, Steward C. Watson

Willian G. Gunderman and R. Ian Kingham, Highway Research Board staff

The sponsoring committee is identified by a footnote on the first page of each report.